A comparison of methods to assess selective disappearance and quantify ageing

Krish Sanghvi[#1], Edward R. Ivimey-Cook[2], Sandra Bouwhuis[3], Irem Sepil*[1], Martijn van de Pol*[4]

[#] *Corresponding author*

** Shared senior authorship*

Affiliations

[1] Department of Biology, University of Oxford, UK

[2] School of Biological Sciences, University of East Anglia, UK

[3] Institute of Avian Research, Wilhelmshaven, Germany

[4] College of Science and Engineering, James Cook University, Townsville, Australia

Contact details

- krish.sanghvi@biology.ox.ac.uk or krishsangvi2007@gmail.com; ORCiD: 0000-0002-5125-2983
- E.Ivimey-Cook@uea.ac.uk; ORCiD: 0000-0003-4910-0443
- sandra.bouwhuis@ifv-vogelwarte.de; ORCiD: 000-0003-4023-1578
- irem.sepil@biology.ox.ac.uk, ORCiD: 0000-0002-3228-5480
- martijn.vandepol@jcu.edu.au; ORCiD: 0000-0003-4102-4079

Abstract

1. Age-dependent change in traits at the population-level can diverge from the within-individual ageing trajectory due to selective disappearance, the biased removal or death of individuals with certain phenotypes.
2. Commonly used methods to assess, and account for, selective disappearance have been developed for relatively simple settings. As such, we currently lack a clear understanding of how well these methods correct for bias when selective disappearance itself is age-dependent, or of their accuracy in quantifying ageing for realistic systems.
3. We use simulations and analytical solutions to quantify and compare how well existing methods (which we term: “additive covariate”, “mean-centring”, and “decomposition”) recapitulate the true ageing trajectory under a range of sampling designs and organismal life-histories. Using two empirical datasets, we further illustrate how the inferred ageing pattern can depend on the specific statistical model used.
4. We show that when selective disappearance is driven by the removal of individuals with distinct ageing trajectories, the decomposition method’s estimate of ageing diverges substantially from the true underlying ageing pattern. Here, the additive covariate and mean-centring methods, which as typically used only account for age-independent selective disappearance (based on an individual’s average quality), are also biased. Mean-centring based models and the decomposition method perform especially poorly when sampling is sparse.
5. Our study quantitatively and systematically synthesizes when and why commonly used methods to quantify ageing might lead to inaccurate conclusions. We suggest that a model where age of last sampling (or lifespan) is included in interaction with

age should be used instead. This model best recapitulates the true ageing trajectory irrespective of organismal life-history, the type of selective disappearance, or missingness in data.

Keywords: aging, frailty, heterogeneity, individual quality, longitudinal vs cross-sectional, senescence

Introduction

What is selective disappearance?

Individuals differ in their resource acquisition (Cam and Monnat, 2000; Reznick et al, 2000) and allocation (Roff and Fairbairn, 2000; van Noordwijk and de Jong, 1986), which can lead to heterogeneity among individuals in the average expression of their life-history and physiological traits, as well as in the ageing trajectories of these traits (Cam et al, 2002; Maklakov and Chapman, 2019). Studies investigating ageing commonly assess, and account for, heterogeneity by modelling the non-independence of repeated measurements from the same individual (Tuljapurkar et al 2009; Vindenes et al 2008). Despite such modelling, unobserved heterogeneity in individual frailty can still bias estimates of ageing through 'selective disappearance'- which arises when individuals' phenotypes co-vary with their likelihood of dying or disappearing from the sampled population (Forslund and Part, 1995; Lailvaux and Kasumovich, 2011; van de Pol and Verhulst, 2006; Vaupel et al, 1979; Vaupel and Yashin, 1985; Wilson and Nussey, 2010; Figure 1A).

Patterns of ageing can vary across individuals, traits, and taxa (Jones et al, 2014; Lemaitre et al, 2024; Sanghvi et al, 2024a), and researchers generally derive information from populations of individuals followed over time in order to infer the true within-individual trajectory of ageing (Baudisch and Stott, 2019; Gaillard and Lemaitre, 2020; Lemaitre and Gaillard, 2017; Nussey et al, 2013; Lemaitre et al, 2020). However, here, selective disappearance can cause the observed or among-individual (cross-sectional) age-specificity of a trait to diverge substantially from the true, within-individual (longitudinal) ageing trajectory (van De Pol and Verhulst, 2006; Rebke et al, 2010). Negative covariances between a trait and lifespan, such as when improvements in a trait comes at the cost of reduced survival, can lead to the selective disappearance of high-quality individuals. In contrast,

positive covariances can lead to the disappearance of low-quality individuals. This might occur when individuals with greater resource acquisition improve multiple traits and their lifespans while individuals with reduced resource acquisition have shorter lifespans as well as poor-quality phenotypes (Sanghvi et al, 2025a; van Noordwijk and de Jong, 1986).

Selective disappearance is pervasive across traits and taxa (e.g. Bouwhuis & Vedder 2017 found selective disappearance for 46% of trait-species combinations in birds). For instance, in several species, individuals with: shorter telomeres (Bichet et al, 2020; Haussmann and Mauch, 2007; Pepke et al, 2023; Power et al, 2025; Salmon et al, 2017); poorer immune function (Beirne et al, 2016; Peters et al 2019; Power et al, 2023); smaller body size (Hamalainen et al, 2014; Hayward et al, 2013; Nussey et al, 2008; Sanghvi et al, 2022); and lower reproductive performance (Lopez-Idiaquez et al, 2016; McClean et al, 2019; Sanghvi et al, 2025b; Sharp and Clutton-Brock, 2010; Thorley et al, 2021), selectively disappear. Selective disappearance is also observed in traits related to social behaviour (Albery et al, 2022; Sadoughi et al, 2024; Moiron & Bouwhuis 2024; Siracusa et al, 2022) and migratory efficiency (Sergio et al, 2014; Wynn et al, 2024). Selective disappearance of low-quality parents can also impact the reproductive success and lifespans of their offspring, potentially buffering deleterious parental age effects (Cansse et al, 2024; Ivimey-Cook and Moorad, 2018; McLean et al, 2019; Moullec et al, 2025; Sanghvi et al, 2024b).

Commonly used methods to assess, and account for, selective disappearance

Studies use three methods primarily (henceforth: 'additive covariate', 'mean-centring', and 'decomposition') for quantifying ageing and selective disappearance. However, these methods have been developed in the last two decades, such that we are only now beginning to appreciate their strengths and limitations. The 'additive covariate' method includes lifespan

(or age at last reproduction, or measurement for non-reproductive traits, hereafter, 'ALR') as an additive term alongside age in a mixed model, to account for age-independent associations between individual removal and average trait expression (Van de Pol and Verhulst, 2006). This method is widely used due to its simplicity (e.g. Bouwhuis et al, 2010a, 2010b; Cope et al, 2022; Froy et al, 2013; Ivimey-Cook and Moorad, 2018; Moullec et al, 2025; Sanghvi et al, 2022). However, it requires lifespan data from a sufficient number of known-aged individuals, which can limit its application.

The 'mean-centring' method partitions the overall, observed, population-level effect of age into an among-individual (the mean sampled age of an individual), and a within-individual component (Δage, i.e. the difference between the sampled age and mean age) (Fay et al, 2022; Van de Pol and Wright, 2009; see Figure 1B). The strength of this method lies in it being able to partition the overall age effect into two processes without requiring data on lifespan (e.g. Bichet et al, 2025; Bouwhuis et al, 2015; Evans et al, 2011; Fay et al, 2021; Sparks et al, 2022; Sun et al, 2025). However, this method has less power to detect within-individual than among-individual age effects when sampling intervals are few (Westneat et al, 2020).

The 'decomposition' method estimates the average, within-individual change in a trait between two successive age classes by comparing the mean values of a trait at those ages, but only of those individuals that are sampled at both ages (Rebke et al, 2010; Figure 1C). Here, the difference in the trait value between the two successive ages directly represents the within-individual change, but only so for that subset of individuals (Martinig et al, 2021; Figure S4). This method is the least used out of the three because it: (i) relies on complete sampling, i.e. nearly all individuals alive being measured at each age, to obtain a representative set of data (Hayward et al, 2013; Hamel et al, 2018; Rebke et al, 2010); and (ii) does not provide statistical testing for the overall effect of age (Hamel et al, 2018; Hayward et

al, 2013). Thus, it is sometimes used in conjunction with the mean-centring or additive covariate methods (e.g. Hamel et al, 2018; Murgatroyd et al, 2018; Nussey et al, 2011; Zhang et al, 2015).

Empirical studies that compare the covariate and mean-centring methods find their conclusions to closely align with each other (Bichet et al, 2022; Gonzalez-Bernado et al, 2025; Kauzulova et al, 2022). However, their agreement with the decomposition method is mixed, with some studies finding similar results (Hamel et al, 2018; Hayward et al, 2013; Nussey et al, 2011) while others reporting discrepancies (Zhang et al, 2014).

Limitations of current methods

An implicit assumption made in all three methods as presented here, is that individuals are disappearing from the population based on their average quality. Specifically, they assume that the bias caused by selective disappearance is *age-independent* and the covariance between trait expression and lifespan (or removal) does not change with age. However, in populations where longer-lived individuals have slower rates of improvement and senescence compared to shorter-lived individuals (Fay et al, 2018; Smallegange and Guenther, 2025; van de Walle et al, 2023), or vice-versa, this assumption can be violated (Hayward et al, 2013; Hamel et al, 2018; Nussey et al, 2008; Zhang et al, 2015). This assumption might also be violated when the direction and magnitude of phenotypic correlations/trade-offs between life-history traits changes with age (Janeiro et al, 2025; Maklakov et al, 2017; Spagopolou et al, 2020; Torres et al, 2011; Figure 1Av-vii, 1Bii-iii). Most studies are agnostic or ignorant towards age-dependence of selective disappearance and to our knowledge, only few have accounted for this (e.g. by including an 'age * ALR' interaction in statistical models: Amininasab et al, 2017; Bouwhuis et al, 2009; Dugdale et al, 2011; Hamel et al, 2018;

Kervinen et al, 2015; McCleery et al, 2008; Moiron and Bouwhuis, 2024; Robinson et al, 2012; Sanghvi et al, 2024b; Torres et al, 2011; Wynn et al, 2025). It therefore remains unknown whether the three methods as typically used by other studies accurately quantify ageing or are subject to potential bias.

A comprehensive theoretical study that benchmarks the three methods on the same dataset, compares them to known ageing trajectories under scenarios of age-independent and age-dependent selective disappearance, and considers a wide range of sampling designs and life-histories is required but currently lacking. Here, we fill this gap using simulations, analytical solutions, and empirical data, to achieve three aims. First, we examine how age-dependent and age-independent selective disappearance cause the among-individual age-specificity of traits to differ from the true within-individual ageing trajectory. Second, we compare results from the three quantitative methods to test which best recapitulates the true ageing trajectory in these scenarios. Third, we quantify the accuracy of these methods across various study designs (e.g. with varying numbers of time steps measured, or missingness of data) and biological systems (e.g. with varying rates and onsets of ageing).

Methods

Parameterization of scenarios

We simulated 27 different scenarios of selective disappearance. Within each scenario, we simulated quadratic reproductive ageing trajectories of 250 individuals per replicate, across 50 replicates of simulated data (unless mentioned otherwise). The age-dependent fecundity of each longitudinally sampled individual was determined using four random variables as:

$$F_{i,\text{age}} = \beta_{0i} + \beta_{1i} \cdot \text{age} + \beta_{2i} \cdot \text{age}^2 \quad \text{for } 1 \leq \text{age} \leq LS_i \tag{1}$$

where LS_i was the individual's lifespan, while the other three variables defined the quadratic ageing trajectory: the intercept (β_{0i}), the linear coefficent (henceforth, 'slope': β_{1i}), and the quadratic coefficient (henceforth, 'shape': β_{2i}). Biologically, the intercept represents the initial (or average, when age is grand-mean centred) fecundity for each individual, while the shape and slope collectively determine the rate of improvement or senescence in early- and late-life (Figure S1). From a specified mean vector and a multivariate normal distribution of these random variables, we independently sampled each of the four traits (T) for every individual as:

$$\boldsymbol{\mu} = [\mu_{LS}, \mu_{\beta_0}, \mu_{\beta_1}, \mu_{\beta_2}]^T \tag{2}$$

$$\boldsymbol{\Sigma} = \begin{pmatrix} \sigma^2_{LS} & \rho_{LS,\beta_0}\sigma_{LS}\sigma_{\beta_0} & \rho_{LS,\beta_1}\sigma_{LS}\sigma_{\beta_1} & \rho_{LS,\beta_2}\sigma_{LS}\sigma_{\beta_2} \\ \rho_{LS,\beta_0}\sigma_{LS}\sigma_{\beta_0} & \sigma^2_{\beta_0} & 0 & 0 \\ \rho_{LS,\beta_1}\sigma_{LS}\sigma_{\beta_1} & 0 & \sigma^2_{\beta_1} & 0 \\ \rho_{LS,\beta_2}\sigma_{LS}\sigma_{\beta_2} & 0 & 0 & \sigma^2_{\beta_2} \end{pmatrix} \tag{3}$$

$$\mathbf{T}_i \sim \mathcal{N}_4(\boldsymbol{\mu}, \boldsymbol{\Sigma}) \quad (4)$$

In Σ, we set the covariances between the slope, shape, and intercepts to zero because we were only interested in isolating the effects of selective disappearance. We parametrized the means in Eq. 4 as: $\mu_{LS} = 25$; $\mu_{\beta_0} = 600$; $\mu_{\beta_1} = 9$; $\mu_{\beta_2} = -0.3$. The coefficient of variation for each random variable was set to 0.2, and minimum lifespan was truncated at one (Figures S2-S5). We independently iterated the correlation between lifespan (LS) and each fecundity trait, i.e. ρ_{LS,β_X}. This gave us three *types* of selective disappearance associated with: (i) the intercept, (ii) the slope, and (iii) the shape. For each type, we varied three magnitudes of correlations: -0.5, 0, or +0.5, to simulate 27 (3^3) different scenarios (Figure S6). Here, non-zero correlations between LS-slope or LS-shape allowed us to simulate age-dependent selective disappearance. Age was simulated as a discrete unitless value (i.e. time step, t).

Simulations were performed using R v4.5.1 (R core team, 2020) and the `MASS::mvrnorm` and `base::matrix` packages were used for Eq. 1-4. We refer to 'fecundity' as the simulated age-dependent trait, but note that this can represent any non-survival, longitudinally measured trait. The complete simulation code and associated data are available at Open science framework https://osf.io/kevnm/overview?view_only=93eba71a58444d19b5fb5287ffbc61e4.

Calculating ageing trajectories

In our first simulation, all individuals alive at a given age were sampled for their fecundity at that age (henceforth, complete sampling-'CS' simulation). Here, after simulating individual-level ageing trajectories, we calculated three additional types of ageing trajectories: (i) 'true', (ii) 'observed', and (iii) 'decomposition'.

True trajectory

The true trajectory represented the expected, average, underlying, within-individual trajectory of ageing across the entire population, free from sampling bias. It was calculated as a deterministic curve generated by directly using the means of the three fecundity variables of the multivariate normal distribution, and was identical across all 27 scenarios and 50 replicates. The fecundity at a given age for this trajectory was calculated as:

$$F_{\text{true,age}} = \mu_{\beta_0} + \mu_{\beta_1} \cdot \text{age} + \mu_{\beta_2} \cdot \text{age}^2 \quad \text{for } 1 \leq \text{age} \leq LS_{max} \tag{5}$$

Observed trajectory

Separately for each replicate within every scenario, we also calculated the observed, population-level ageing trajectory across sampled individuals. At each age, the observed fecundity ($\bar{F}_{\text{obs,age}}$) of living individuals, was calculated as:

$$\bar{F}_{\text{obs,rep,age}} = \frac{1}{N_{\text{rep,age}}} \sum_{i|LS_i \geq \text{rep,age}} F_{i,\text{rep,age}} \tag{6}$$

where $N_{\text{rep,age}}$ was the number of sampled individuals. For a given age, this value was then averaged across 50 replicates within each scenario and the observed trajectory was constructed by calculating $\bar{F}_{\text{obs,age}}$ across all sampled ages. Mortality and sampling design altered the composition of the population over time, thus, the observed trajectory reflected consequences of selective disappearance (Supplementary section S1) and methodology (see below).

Decomposition trajectory

We calculated age-dependent change in fecundity as described by the decomposition method (Rebke et al, 2010). For each discrete age interval $[\text{age}, \text{age} + 1]$, we identified the subset of individuals alive and sampled at both ages. The 'decomposed' mean within-individual change in fecundity for this interval, I_{age}, was calculated as: $I_{\text{age}} = \overline{F}_{\text{age+1}} - \overline{F}_{\text{age}}$, where $\overline{F}_{\text{age+1}}$ and $\overline{F}_{\text{age}}$ represent the mean fecundity at the two ages, calculated strictly for the subset of individuals that survived to age + 1 (i.e. $F_i \mid LS_i \geq \text{age} + 1$). The full trajectory was then reconstructed

cumulatively. We defined the starting value, $\hat{F}_{\text{start}}$, as the mean fecundity of the subset of individuals observed at the first utilizable age ($\text{age}_{\text{start}}$) who were also sampled at the next age. Fecundity at subsequent ages was estimated by adding the cumulative interval changes to this baseline:

$$\hat{F}_{\text{age}} = \hat{F}_{\text{start}} + \sum_{j=\text{age}_{\text{start}}}^{\text{age}-1} I_j \tag{7}$$

Sparse sampling

In addition to the CS simulation, we created three distinct types of simulations to separately test the impact of three types of missingness in data (Aim 3).

Missing completely at random

We simulated individuals to be missing completely at random (henceforth, 'MCAR' simulation) at each time step, which in empirical studies might be due to stochastic capture/recapture rates. To do this, we first generated a complete sampling dataset as described above. We then subsampled this dataset to create missingness by subjecting each time step of every individual, independently, to a Bernoulli trial with a retention probability of 0.5. We doubled the number of simulated individuals in each replicate of the MCAR simulation to 500 to maintain sample sizes comparable to the CS simulation at each age.

Age-dependent missingness

We simulated a dataset where older individuals were less likely to be sampled (henceforth, missing when old-'MWO' simulation). Biologically, this could represent right censoring caused by the termination of a study or conducting of analysis before all individuals die, low recapture rates of old individuals, or higher rates of skipped breeding and reproductive failure in old individuals (see Bouwhuis et al, 2012; Zhang et al, 2015).

We also simulated a dataset where younger individuals were less likely to be sampled (henceforth missing when young-'MWY' simulation). Biologically, this could represent low capture rates of young individuals caused by their temporary dispersal/migration or reduced boldness, or the

study commencing later than the birth/sexual maturity of many individuals. For the MWO and MWY simulations, we modeled 500 individuals per replicate.

To create age-dependent missingness, we first generated a complete dataset as described above, which was then subsampled with the probability of retaining data at each time step for every individual, '$P(\text{keep})_{\text{age}}$', determined by a logistic function:

$$P(\text{keep})_{\text{age,MWO}} = \frac{1}{1 + \exp[k(\text{age} - a_m)]} \tag{8}$$

and,

$$P(\text{keep})_{\text{age, MWY}} = 1 - \frac{1}{1 + \exp[k(\text{age} - a_m)]} \tag{9}$$

where a_m represented the age at which the sampling probability was 50%; and k was the steepness of the sampling probability around the midpoint. A data point was only retained if a random number drawn from a uniform distribution between 0 and 1 was less than $P(\text{keep})_{\text{age}}$ for that observation. We set $a_m = 40$ for the MWO simulation, and $a_m = 10$ for the MWY simulation to produce a symmetrical but inverse function around the mean lifespan of 25 timesteps (Figure S7).

For the MCAR, MWO, and MWY simulations, the constructed 'decomposition' and 'observed' trajectories only used the respective sub-sampled data.

Calculating deviation from the true trajectory

For every simulated age, we estimated the deviation between: (i) the observed ($\bar{F}$) and the true fecundity (F_{true}) as '$D_{\text{Obs,age}}$' (Aim 1); and (ii) the decomposition ($\hat{F}$) and the true fecundity as '$D_{\text{Deco, age}}$' (Aim 2; also see Figure 1D):

$$D_{\text{Obs,age}} = \frac{1}{N_{\text{rep}}} \sum_{\text{rep}=1}^{50} \frac{\bar{F}_{\text{rep, age}} - F_{\text{true, age}}}{F_{\text{true, age}}} \times 100 \tag{10}$$

and:

$$D_{\text{Deco, age}} = \frac{1}{N_{\text{rep}}} \sum_{\text{rep}=1}^{50} \frac{\hat{F}_{\text{rep, age}} - F_{\text{true, age}}}{F_{\text{true, age}}} \times 100 \tag{11}$$

This was done independently for every replicate in each of the 27 scenarios, and separately for the four simulations (i.e. CS, MCAR, MWO, MWY). For each simulated age, this value was then averaged across the 50 replicates within each scenario.

Importantly, we analytically solved how the observed and decomposition trajectory deflected from the true trajectory (full derivation in Supplementary section S1).

Comparison of statistical models

We fit six Linear Mixed-Effects Models (LMMs) to the sampled data using the package `lme4::lmer` with a Gaussian error distribution. Each model was fit separately on data within each replicate and scenario, and separately for the four simulations. All models included a random intercept for unique individual ID (u_{0i}) and a residual error term (ϵ_{it}), and were fit using maximum likelihood to allow comparisons of different fixed effect structures.

Model descriptions

The fecundity F_{it} of individual i at measurement occasion t was modeled as a function of the individual's age at that time (age_{it}) as follows:

Model 1: Negative control not accounting for selective disappearance.

$$F_{it} = \beta_0 + \beta_1 \text{age}_{it} + \beta_2 \text{age}_{it}^2 + u_{0i} + \epsilon_{it} \tag{12}$$

Model 2: The 'additive covariate' model with ALR (representing age at last sampling) as an additive term (van de Pol and Verhulst, 2006).

$$F_{it} = \beta_0 + \beta_1 \text{age}_{it} + \beta_2 \text{age}_{it}^2 + \beta_3 \text{ALR}_i + u_{0i} + \epsilon_{it} \tag{13}$$

Model 3: The 'mean-centering' model (van de Pol and Wright, 2009; Fay et al, 2021) that separates the observed trajectory into among- ($\overline{\text{age}}_i$) and within-individual components (Δage or '$\text{age}_{it} - \overline{\text{age}}_i$').

$$F_{it} = \beta_0 + \beta_1(\text{age}_{it} - \overline{\text{age}}_i) + \beta_2(\text{age}_{it}^2 - \overline{\text{age}^2}_i) + \beta_3\overline{\text{age}}_i + u_{0i} + \epsilon_{it} \quad (14)$$

Model 4: An extension of Model 2, with an interaction between the age terms and ALR.

$$F_{it} = (\beta_0 + \beta_1\text{age}_{it} + \beta_2\text{age}_{it}^2) + (\beta_3 + \beta_4\text{age}_{it} + \beta_5\text{age}_{it}^2) \cdot \text{ALR}_i + u_{0i} + \epsilon_{it} \quad (15)$$

Model 5: An extension of model 3, with $\overline{\text{age}}$ and Δage terms interacting.

$$\begin{aligned} F_{it} = \beta_0 + \beta_1(\text{age}_{it} - \overline{\text{age}}_i) + \beta_2(\text{age}_{it}^2 - \overline{\text{age}^2}_i) \\ + [\beta_3 + \beta_4(\text{age}_{it} - \overline{\text{age}}_i) + \beta_5(\text{age}_{it}^2 - \overline{\text{age}^2}_i)] \cdot \overline{\text{age}}_i + u_{0i} + \epsilon_{it} \end{aligned} \quad (16)$$

Model 6: A positive control fitting 'lifespan' as the interactive covariate.

$$F_{it} = (\beta_0 + \beta_1\text{age}_{it} + \beta_2\text{age}_{it}^2) + (\beta_3 + \beta_4\text{age}_{it} + \beta_5\text{age}_{it}^2) \cdot \text{LS}_i + u_{0i} + \epsilon_{it} \quad (17)$$

Model fit, accuracy and precision

We estimated the Akaike information criteria (AIC) for each model and used the average AIC across 50 replicates to compare models within each scenario and simulation type (Aims 2). A ΔAIC of ≥ 2 was interpreted as a worse model support.

To compare the accuracy of different models, we used the 'predict' function (*car* package) to estimate the age-effect on fecundity ($F_{\text{model,age}}$) as predicted by each statistical model. Then, at each age and separately for each model in every scenario and simulation dataset, we calculated the relativized difference between the mean predicted fecundity value (across 50 replicates) of the model and the true trajectory as:

$$D_{\text{model, age}} = \frac{1}{N_{\text{rep}}} \sum_{\text{rep}=1}^{50} \frac{F_{\text{model, rep, age}} - F_{\text{true, age}}}{F_{\text{true, age}}} \times 100 \quad (18)$$

We also calculated the variance in each model's prediction and in the decomposition method's estimated fecundity, to compare the precision of these models and methods (Supplementary section S2).

Random slopes

Random slopes are sometimes included in statistical models to account for among-individual heterogeneity in ageing trajectories. To demonstrate that random slope terms do not account for age-dependent selective disappearance (Aim 2), we created a separate simulation. Here, we compared models 1-5 containing only a random intercept term, 'u_{0i}', against models containing the same fixed effects but additionally containing a random slope term '$u_{1i}\text{age}_{it}$' (representing the product of individual i's constant deviation from the mean slope u_{1i} and the individual's changing age at each sampling point, t). For simplicity and due to sufficiency, we simulated ageing trajectories as linear. Consequently, the 10 models fit to these data did not contain a quadratic age term. As proof of concept, we only simulated three scenarios under complete sampling- (i) no selective disappearance, (ii) selective disappearance linked with intercept only, (iii) selective disappearance linked with slopes only. Lifespans, intercepts, and slopes were sampled from a multivariate distribution as described in Eq. 1-4 (however, excluding the shape variable). Here, μ_{β_1} was parameterized as -6 and σ_{β_1} as 1.2, to represent a life-history where senescence onsets in early-life without improvements in fecundity (Aim 3).

Sensitivity analyses

We further tested how various biological and methodological attributes impacted our results (Aim 3): (i) the specific parameterization of the slope and shape, thus, the rate and onset of ageing; (ii) the sample size; (iii) the distribution of lifespan (thus mortality rates); and (iv) the number of simulated time-steps (a proxy for species' lifespan or sampling design). Detailed descriptions of these sensitivity analyses can be found in Supplementary section S3 (also see Figure 1E, Figures S8-S10).

Empirical demonstration

To test whether the commonly used models 2 and 3 lead to distinct inferences about ageing compared to the seldom used models 4 and 5 in empirical systems, we re-analyzed data from two studies. One contained data on the fecundity of lab-adapted female fruit flies across their lifetime (Sanghvi et al, 2025b). The other dataset was obtained from a long-term study on a wild population of great tits (Bouwhuis et al, 2009) and contained data on a phenological trait (egg laying date) that was not analyzed in the original study. We fit models 1-5 to both datasets, compared model AICs, and visualized their predictions for the effects of age. We also included relevant environmental and treatment variables as suggested within each corresponding study. More details can be found in Supplementary section S4.

346 # Results

347 ***How do trajectories deviate?***

348 In our simulation with complete sampling of individuals and normally distributed lifespan
349 with an average of 25 time steps, (i.e. `CS' simulation), the 'observed' population-level
350 ageing trajectory of the trait closely matched the 'true' within-individual trajectory in the
351 absence of selective disappearance (Figure 2A). As expected, in this simulation, selective
352 disappearance linked with the intercept (Figure 2B-C), slope (Figure 2D-E), and/or shape
353 (Figure 2F-I) of the trait, led to substantial deviations between the observed and true
354 trajectories in mid- and late-life (Figure S11, S12, S13). This led to either an over- or under-
355 estimation of the true ageing pattern, depending on the sign of each correlation with lifespan
356 (Aim 1). Importantly, even when selective disappearance was not linked with the trait's
357 intercept, but with the trait's slope and/or shape, the observed ageing trajectory deviated
358 substantially from the true trajectory (often by >50%- Figure 2D-G). The decomposition
359 trajectory matched the true trajectory under no selective disappearance as well as under
360 selective disappearance linked with the trait's intercept (Aim 2, Figure 2A-C). However,
361 when selective disappearance was linked with trait's slope and/or shape, the decomposition
362 method produced biased results that were particularly substantial in late-life (up to 40%;
363 Figure 2D-I, S11, S12; also see analytical solutions for an explanation).

364

365 ***How well do statistical models perform?***

366 In our CS simulation, models 4 (included a two-way interaction between ALR and age) and 5
367 (included an interaction between the $\overline{age}$ and Δage terms) had lower AICs than other models
368 across all scenarios (Figure 3, Figure S14). Under complete sampling, models 4 and 5 had

identical AICs because mean age, ALR, and LS were perfectly correlated (Pearson's r = 1; also see Fay et al, 2022) (Aim 2).

In the CS simulation across scenarios where selective disappearance occurred, the deviation of predictions of models 4 and 5 from the true trajectory was slightly greater (0% to 4%) compared to that of the decomposition method (0% to 2%), in early-life (Aim 2; Figure 4, Figure S15). However, in mid- and late-life, especially in scenarios where selective disappearance was linked with the slope and/or shape (Figure 4D-I), the decomposition method deviated substantially more from the true ageing trajectory (up to 40%) than predictions from models 4 and 5 did (0% to 10%) (Figure S16). There was no substantial penalty on the precision of models 4 and 5 despite them having more parameters being estimated than other models (Figure S17). Our sensitivity analyses (Figure 1E; Aim 3) parameterized for: faster or slower rates of ageing (Figure S18 to S25), short-lived species (Figure S26 to S28), or a reduced sample size (Figures S29, S30), produced qualitatively similar results to our CS simulation as described above.

We also simulated linear trajectories of ageing to represent an early onset of senescence without improvements in trait (Aim 3), and here, compared models with or without random slopes (Aim 2). As expected, the five models that only contained random intercepts (Figure 5A-C) performed worse than their corresponding models that additionally included random slopes (Figure 5D-F). Under selective disappearance linked to the trait's slope, models 4 and 5 outperformed models 1-3, but simply modelling a random slope term was insufficient to account for bias (Figure 5C vs 5F). Even under the absence of selective disappearance, the interaction models (4 and 5) provided a better fit to the data when neither of the five models included a random slope term (Figure 5B). However, when random slopes were included in a scenario without selective disappearance, all five models performed equally well (Figure 5E). These results demonstrate that a random slope term does not

account for age-dependent selective disappearance, however, the interaction terms in models 4 and 5 partly account for among-individual heterogeneity in ageing when a random slope term is not modelled (Figure 1A).

The influence of missingness of data

Missing completely at random

In the MCAR simulation where 50% of data was missing completely at random, deviations between the observed and true trajectories under selective disappearance were qualitatively similar those obtained from the CS simulation (Aim 3; Figure S31, S32). Similarly, the decomposition method produced bias at old ages when selective disappearance was linked with slopes or shapes (Figure S31, S32). In contrast to our findings from the CS simulation, in the MCAR simulation, model 4 fit the data better than models 1, 2, 3, and 5 (Figure 6, Figure S33). This was because $\overline{age}$ was a poorer proxy of LS (r = 0.852) than ALR was (r = 0.962; Figure S34). Comparisons of model 4's predictions and of the decomposition trajectory, to the true trajectory, yielded similar patterns as seen in the CS simulation above (Figure S35). Even for the shorter-lived species (μ_{LS} = 5 time steps) (Figures S36-S38), results for the deviation between trajectories and for model comparisons closely mirrored results for the long-lived species described above.

Age-dependent missingness

When old individuals were more likely to have missing data (i.e. MWO simulation), our results differed from those in our CS simulation in one key way- model 4 fit the data slightly better than models 1, 2, 3, and 5 across all scenarios (Aim 3; Figure S39-S44). This was

because ALR-LS had a slightly stronger correlation (r = 0.998) than $\overline{age}$-LS (r = 0.994) (Figures S40-S42). This difference between models 4 and 5 was exacerbated when young individuals had higher missingness (i.e. MWY simulation), because here, the correlation between ALR-LS was substantially stronger (r = 0.999) than between $\overline{age}$-LS (r = 0.942) (Figure S45-S47). In the MWY simulation, the decomposition trajectory was less precise at young-ages compared to its precision in the CS simulation (Figure S48).

Alternative lifespan distributions

The sampling of lifespan from right-skewed Gamma distributions (to represent high early-life mortality), simulated separately for complete and missing-completely-at-random sampling designs, produced similar results to those described above, irrespective of the number of mean time steps (i.e. species' lifespan) simulated (Figure S49-S52).

Empirical implementation

We re-analyzed data from two published studies (Bouwhuis et al, 2009; Sanghvi et al, 2025b) to demonstrate how our theoretical results apply to empirical data, and investigate whether the 'additive covariate' or 'mean-centring' models (Models 2 and 3) lead to distinct predictions compared to the interaction models (Models 4 and 5) in real datasets.

Our reanalysis of the fruit fly dataset containing data on female fecundity, showed that model 4 provided the best fit to the data, and a better fit than the originally used model 2 (ΔAIC compared to model 4, of models 1, 2, 3, and 5 = 38.4, 24.1, 11, 6.2, respectively; Figure 7A). Model 4 predicted a shallower senescence in late-life compared to predictions from other models (Table S1). This was because individuals that lived longer not only had

lower average fecundity (as reported in the original study), but also had shallower rates of senescence (Figure 7B; Table S1).

Our analysis of female egg laying date and its ageing in great tits similarly revealed that model 4 provided a better fit to the data compared to the other models (ΔAIC compared to model 4, of models 1, 2, 3, and 5 = 11.8, 9.5, 13.8, 15.7 respectively; Figure 7C). Model 4 predicted a shallower delay in laying date in late-life compared to other models (Table S2; Figure 7C, 7D). This was because longer-lived individuals had a shallower advance in laying date in early-life, but also a shallower delay in laying date at older-ages.

Analytical solutions

Our analytical solutions provided three important insights (fully presented in Supplementary section S1). First, the deviation between the observed and true pattern at a given age due to selective disappearance depends on the product of two processes: the mortality hazard and the overall covariance between lifespan and fecundity at that age. Here, the observed trajectory deviates from the true trajectory because the individuals that survive either, (i) do not have the same age-independent quality (i.e. differ in intercept), or (ii) do not have the same ageing pattern (i.e. differ in their slope or shape) (Figures S53-S55). Due to LS-shape and LS-slope correlations being scaled by age, age-dependent selective disappearance produces a greater bias in later-life. Importantly, selective disappearance of the intercept can lead to a bias that is entirely independent of individual-level ageing (e.g. observing population-level ageing despite individuals themselves not ageing).

Second, there is an inaccuracy associated with the calculation of the decomposition method. This method successfully removes bias caused due to intercept-LS correlations (i.e. age-independent selective disappearance) and due to changing mortality rates. However, it

464 mathematically cannot remove bias caused by age-dependent selective disappearance linked
465 to the slope or shape (Figure S56; Supplementary section S1.3), such that at later ages, it
466 produces an inaccurate estimate of the ageing trajectory. The deviation of the observed
467 population-level ageing trajectory includes this same bias, but additionally includes a bias
468 related to the acceleration of selection on mortality as age increases. Third, the absolute
469 magnitude of selective disappearance at a given age does not depend on the among-individual
470 variability in lifespan, σ_{LS}, but depends on the variability of the three fecundity variables
471 (intercept, slope, shape). However, the rate of change of the deviation over time depends
472 inversely on σ_{LS} (Figure S57, S58; Supplementary section S1.4).

473

474 # Discussion

475 **Aim 1: Age-dependent selective disappearance**

476 The covariance between lifespan and slope or shape at a given age determines the age-
477 dependent component of selective disappearance, whereas the covariance between lifespan
478 and intercept determines the age-independent component. Our simulations show that age-
479 dependent selective disappearance driven by the removal of individuals with distinct ageing
480 trajectories in a trait can bias estimates of the true, underlying ageing pattern. This occurs
481 even when selective disappearance linked with the trait's intercept is absent or accounted for
482 and becomes especially problematic at later ages.

483 There are several biologically plausible reasons for why age-dependent selective
484 disappearance might manifest (Figure 1Av-vii, 1Biii). The ageing trajectory may co-vary with
485 lifespans if individuals in a population differ in their pace-of-life syndromes (Hayward et al,
486 2013; Hamel et al, 2018; Healy et al, 2019; Reale et al, 2010; Torres et al, 2011). Specifically,
487 if individuals that die earlier also display steeper rates and early onset of senescence in other

traits, older age classes will be increasingly composed of organisms with shallower rates and later onset of senescence (Figure S6). Age-dependent selective disappearance could also manifest due to condition-dependence. For example, if the survival cost of expressing/improving a trait at a young age is low for all individuals, everyone might be able to express the trait equally well, leading to a shallow covariance between the trait and lifespan in early-life (Johnson and Gemmell, 2012). However, at old ages, if the cost is low only for individuals of better condition, here, longer lived individuals might express the trait more than soon-to-die individuals, causing the association between this condition-dependent trait and lifespan to be age-dependent (Brooks and Kemp, 2001; Hansen and Price, 1995; Kokko, 1998; Sanghvi et al, 2024b).

When the measured trait relates to reproduction, age-dependent selective disappearance could manifest in three additional ways. First, it could represent changing selection gradients on lifespan with age. Donertas and Partridge (2025) show this, whereby selection on lifespan is positive and steep at young ages. However, at older ages, selection is shallow (Figure S59, S60)- a pattern that is consistent with the force of selection weakening with age due to extrinsic mortality, resulting in a 'selection shadow' (Hamilton, 1966; Lemaitre et al, 2024; Maklakov and Chapman, 2019; Williams, 1957). Second, trade-offs between somatic repair and reproduction might generate age-dependent selective disappearance (Chen et al, 2020; Lemaitre et al, 2015, 2024; Maklakov and Chapman, 2019). At young ages, accumulated damage is lower, which could lead to the costs of reproduction on lifespan being buffered. However, at old ages, such costs might be greater because somatic damage has accumulated (Kirkwood and Rose, 1991) leading to LS-reproduction covariances becoming more negative with age. Third, terminal investment, where individuals allocate greater resources to reproduction at the expense of survival at later, but not at earlier ages, due to residual lifespans reducing with age (Duffield et al, 2017; Reed et al, 2008), might

cause lifespan-reproduction correlation to become more negative with advancing age (Figures S59, S60).

Aims 2 and 3: Comparison of methods across a variety of systems

Additive vs. interactive, mean-centring vs. covariate models

We compared the performance of two commonly used models (i.e. the 'additive covariate' model 2, and the 'mean-centring' model 3) to that of seldom used 'interaction' models (4 and 5). These models differed in whether they were able to account for age-dependence of selective disappearance. Unsurprisingly, the additive models produce biased estimates of the ageing pattern when selective disappearance is age-dependent (i.e. due to LS-slope or LS-shape correlations). In such scenarios and under no missingness of data, both the interaction models (4 and 5) produce identical estimates of the true trajectory (also see Fay et al, 2022) and outperform other models. However, under incomplete sampling (especially MCAR and MWY), we found that model 4 (included an interaction between ALR and age terms) consistently outperformed other models, including model 5 (included an interaction between $\overline{\text{age}}$ and Δage terms). Our reanalyses of two empirical datasets from Bouwhuis et al (2009) and Sanghvi et al (2025b) exemplified this pattern, where model 4 provided the best fit to the data and a substantially different prediction of the late-life ageing trajectory compared to other models.

The differences between models 4 and 5 arise because under all three simulated missingness scenarios, ALR is a better proxy of lifespan than mean age is. The error associated with ALR as a proxy for lifespan only depends on the rate of missingness, rather than the length of the lifespan itself. For example, under 50% missingness, ALR deviates from true lifespan by a constant, small, expected value (approximately one time step),

regardless of whether the individual lives for 5 or 25 time steps (Figures S34 and S38). In contrast, mean age is a centroid metric. Its error rate scales with lifespan, and its calculation is highly sensitive to among-individual heterogeneity in sampling regularity which introduces stochasticity (further explained in Figures S34, S38, S61).

Model 4 vs. decomposition method

Our results highlight some key differences between model 4 (which consistently outperformed other models) and the decomposition method. In nearly all scenarios and simulations, in early-life, the decomposition method generally provides a slightly better (typically < 3%) recapitulation of the true ageing trajectory compared to model 4. However, in mid- and late-life, the decomposition method performs substantially worse (up to 50% deviation in several cases) especially under the 24 scenarios with age-dependent selective disappearance. There are two likely explanations for this. First, in early life and under complete sampling, sufficient numbers of individuals are sampled at successive time-steps, thus cohort averages provide a precise estimate of within-individual change. However, once mortality accelerates in later-life, sample size for successively sampled individuals necessarily gets lower, causing imprecision of the decomposition method. Missingness of data further exacerbates this exponentially (Hamel et al, 2018; Hayward et al, 2013; Nussey et al, 2011), for example, under random missingness with a probability of P, the likelihood of sampling an individual at two successive ages becomes P^2. Second, our analytical solutions reveal a previously unknown bias in the decomposition method- it implicitly assumes that the rate of ageing is the same for individuals that survive and those who disappear. When selective disappearance is linked with the trait's slope or shape, this assumption creates a bias

that accelerates with age, making the decomposition method less useful in quantifying senescence (Figure S57, S58 and Supplementary section S1.3).

Guidelines for empiricists

Whenever possible, we suggest that researchers fit parametric ageing curves separately for each individual and then calculate the average coefficients (e.g. intercept, slope, and shape) of these curves. These average coefficients can provide a parametric approximation of the true within-individual ageing trajectory; however, this approach should be used only for continuous traits and large datasets. Currently, when lifespan data are incomplete, researchers tend to use the mean-centring method by calculating the mean and delta age variables from the sampled time steps. However, we demonstrate that ALR provides a better proxy for lifespan than mean age, even under several types of missingness. Contrary to common practise, we thus recommend that model 4 (where ALR represents the age of last sampling/observation) be preferred over model 5, or at least their performance be compared when analysing datasets with missingness. Here, empiricists could further quantify and report: (i) whether missingness in their data is age- or trait-dependent (e.g. Bouwhuis et al, 2012; Mittell et al, 2025); and (ii) the strength of correlation between ALR and mean age. Importantly, we recommend that studies use the interaction model (model 4) as their "global" model whenever possible and only use the additive model (model 2) when the interaction terms are not significant and not of biological interest.

If the data do not allow using the interaction models due to overfitting or convergence issues, we recommend several visualisations to qualitatively infer the presence and type of selective disappearance. First, the influence of age on a specific trait could be visualised by grouping into different ALR bins (e.g. Figure 1A, 1B, 6B, 6D). Here, under no selective

584 disappearance, the different bins should overlap substantially or fluctuate randomly. Under
585 age-independent selective disappearance (linked with intercept), the shape of each bin's
586 trajectory will be similar, but its average value will be consistently different. However, under
587 age-dependent selective disappearance (linked with slope or shape), each bin will display a
588 distinct trajectory of ageing with a systematic increase or decrease between the bins as age
589 progresses. Second, we suggest visualising the correlation between lifespan (or ALR) and the
590 sampled trait at each age. If the coefficients of these associations systematically change with
591 age, this likely indicates that selective disappearance is age-dependent (e.g. Figure S59, S60).

592 Our simulations represent idealised datasets in which: individuals follow quadratic,
593 parametric ageing trajectories; measurement error is absent; missingness is independent of
594 condition; environmental influences are not included; traits are sampled from continuous
595 distributions; lifespan and the sampled trait are linearly related at a given age; LS-β_x
596 correlations are high; and the true ageing trajectory is known. These modelling choices were
597 made to enable clear interpretation of results and facilitate implementable recommendations,
598 but they inevitably have limitations. We addressed some of these limitations by: (i)
599 demonstrating that insights from our simulation are applicable to empirical datasets, and (ii)
600 providing analytical solutions that generalise our results across a range of parameterizations
601 (Supplementary Section S1; Figure S53-S56). Empiricists can further address some of these
602 limitations. For example, ALR could be included as a non-linear (e.g. quadratic) term if
603 individuals with medium lifespans are of a higher quality than individuals with the lowest or
604 highest lifespans (Balbontin et al, 2007; Nussey et al, 2006, 2009, 2011; Reid et al, 2003;
605 Simons et al, 2016). Generalized additive mixed-effects models containing a tensor product
606 smooth between ALR and age (e.g. in R's *mgcv* package), rather than ALR being included as
607 a parametric linear term (e.g. Cooper et al, 2021; Hamalainen et al, 2014; Sanghvi et al,
608 2021), could also be fit on large datasets. Our approach could also be extended to model

selective appearance- the entering of individuals in a dataset being biased based on the phenotype, by simply replacing the ALR term with AFR (age at first sampling).

The concept of selective disappearance can manifest in systems or at levels of biological organisation that are not typically considered. For instance, sperm cells that are sampled later within stored ejaculates could represent a biased sperm phenotype due to selective death of poor-quality or rapidly senescing sperm (Alavioon et al, 2017; Marcu et al, 2024; Sanghvi et al, 2025c). Furthermore, reaction norms might selectively disappear across an environmental gradient, such that in more extreme environments, sampled individuals are those with steeper or shallower reaction norms (Fay et al, 2022). In studies where individuals mate sequentially with several partners, those with higher mating success might also have a higher reproductive output with each mate, compared to individuals that only mate with few partners (e.g. Sanghvi et al, 2025d). This would lead to later matings containing a biased sampling of reproductive phenotypes (Sanghvi et al, 2025e). Thus, quantifying and accounting for selective disappearance has implications beyond just ageing research, and researchers analysing any longitudinal data should be cautious of such processes biasing their results.

Figures

Figure 1: Conceptual diagram explaining our study aims. (A) Heterogeneity among individuals (here represented as three hypothetical individuals- colours) can occur in their intercepts or their rates of ageing (represented here as slopes) (top row). Additionally, individuals can differ in their lifespans, and its covariance with individual intercepts and/or slopes can lead to age-independent and age-dependent selective disappearance, respectively (bottom row). **(B)** Four hypothetical individuals' quadratic ageing patterns (dashed blue, green, pink, grey curves), and their mean age of sampling (corresponding-coloured circle) are shown. The mean-centring method partitions the among- (mean age- solid brown) from the average, within-individual (Δage- solid black) effect of age. Here, an interaction between the mean age and Δage terms represents age-dependent selective disappearance **(C)** The decomposition method considers only the subset of individuals sampled at two successive time steps to estimate the average within-individual change over that time step. **(D)** Nine hypothetical individuals (gray) differ in their intercepts and lifespans, with covariance between these leading to age-independent selective disappearance. Here, the observed, population-level ageing trajectory (orange) differs from the true within-individual trajectory (solid black), which at a given time step *t*, can be represented as the relativised deviation between the observed and true pattern as: (*y1-y2*)*100/*y2*. **(E)** Cartoons depicting the different scenarios considered in the sensitivity (from left to right): species' onset of senescence, pace of life, types of data missingness, sample sizes, and lifespan distributions.

Figure 2: The relativised deviation caused by selective disappearance in our CS simulation depends on the type and magnitude of selective disappearance. Orange curves shows the relativised deviation between the observed (cross-sectional) versus true (within-individual) trajectory; purple curves, that between the decomposition and true trajectory, averaged across 50 replicates. Black (dashed) curve shows the analytical calculation of the relativised deviation between the observed versus true trajectory. Facet titles show the pairwise correlations between LS and each fecundity variable. The vertical dotted line shows the true age of onset of senescence in fecundity. For simplicity, only 9 scenarios are shown, but all 27 considered scenarios presented in Figures S11 and S12.

Figure 3: Support by the data (ΔAIC compared to best model) for models 1-5 in the CS simulation. For simplicity, only 9 scenarios are shown but all 27 presented in Figures S14 and S15. Facet titles show the pairwise correlations between LS and each of the three fecundity variables (intercept, slope, shape).

Figure 4: Comparison of model/method predictions for the effects of age on fecundity reveals that model 4 generally outperforms other models. Relativised difference between predictions from the statistical models 1-5 and the true trajectory, as well as between the decomposition and the true trajectory, for data generated in the CS simulation.

Figure 5: Models containing random slopes fit the data better than models with only random intercepts. Three scenarios of selective disappearance shown as facets, and the Y axis shows ΔAICs compared to the best fitting model that contains the same random effects within each scenario. Models in the top and bottom plots are fitted to the same data and identical in their fixed effect structures. However, models in the top row contain only a random intercept term while models in the bottom row contain a random intercept and random slope term. Numbers show the models' raw AIC values.

Figure 6: Models 4 outperforms model 5 when data are missing. Comparison of ΔAICs of models 1-5 to the best fitting model in that scenario, fitted on data simulated in the MCAR simulation. For simplicity, only 9 scenarios shown but all 27 considered scenarios presented in Figures S33 and S35. Unlike in the CS simulation (Figure 3), here, models 4 and 5 are not analogous.

Figure 7: Re-analysis of two empirical studies shows that age-dependent selective disappearance manifests in real-world datasets, where model 4 provides the best fit to these data. (A) Model predictions (log scale due to negative binomial error distribution) for the effect of age from the five statistical models fit to a fruit fly dataset. The best fitting model 4 (containing 'age * ALR + age^2 * ALR'), predicts a shallower senescence in late-life compared to other models. **(B)** Age-dependent selective disappearance manifests as the difference in fecundity between different lifespan bins to increase with age. **(C)** In a great tit dataset, the best fitting model 4 predicts a shallower delay in laying date in late-life compared to other models. **(D)** This is because longer- and shorter-lived individuals have distinct trajectories of age-dependent changes in their laying date.

Contributions

Conceptualisation: KS, MVDP, EIC, SB, IS
Methodology: KS, MVDP, EIC, SB, IS
Formal analysis (simulation): KS
Formal analysis (analytical): KS, MVDP
Writing (original draft): KS
Writing (revision): MVDP, SB, EIC, IS

Data and code accessibility statement

Entire simulation code and HTML output, along with all associated empirical data are available at Open science framework https://osf.io/kevnm/overview?view_only=93eba71a58444d19b5fb5287ffbc61e4 under an anonymized link.

Funding

IS was supported by a Biotechnology and Biological Sciences Research Council Fellowship (BB/T008881/1) and the Royal Society (Dorothy Hodgkin Fellowship: DHF\R1\211084).

Acknowledgements

We are deeply grateful to Remi Fay, Joel Pick, Jean-Michel Gaillard, and Samuel Gascoigne for discussions and suggestions at early stages. We thank Ben Sheldon for permission to use and re-analyse the great tit data which is a part of the Wytham woods long-term study, and all students and field workers who contributed to that dataset.

Conflict of interest

Authors declare no conflicts of interest.

Use of AI statement

Google AI's Gemini 3.0 Pro was used to correct syntax errors in the R script, and to develop code for the Gaussian copula method in the Gamma distribution simulation. The corresponding author KS has ensured the accuracy of the code when using AI and takes full responsibility for it.

References

Alavioon, G., Hotzy, C., Nakhro, K., Rudolf, S., Scofield, D. G., Zajitschek, S., Maklakov, A. A., & Immler, S. (2017). Haploid selection within a single ejaculate increases offspring fitness. *Proceedings of the National Academy of Sciences*, *114*(30), 8053–8058. https://doi.org/10.1073/pnas.1705601114

Albery, G. F., Clutton-Brock, T. H., Morris, A., Morris, S., Pemberton, J. M., Nussey, D. H., & Firth, J. A. (2022). Ageing red deer alter their spatial behaviour and become less social. *Nature Ecology & Evolution*, *6*(8), 1231–1238. https://doi.org/10.1038/s41559-022-01817-9

Amininasab, S. M., Hammers, M., Vedder, O., Komdeur, J., & Korsten, P. (2017). No effect of partner age and lifespan on female age-specific reproductive performance in blue tits. *Journal of Avian Biology*, *48*(4), 544–551. https://doi.org/10.1111/jav.00970

Balbontín, J., Hermosell, I. G., Marzal, A., Reviriego, M., De Lope, F., & Møller, A. P. (2007). Age-related change in breeding performance in early life is associated with an increase in competence in the migratory barn swallow *Hirundo rustica*. *Journal of Animal Ecology*, *76*(5), 915–925. https://doi.org/10.1111/j.1365-2656.2007.01269.x

Baudisch, A., & Stott, I. (2019). A pace and shape perspective on fertility. *Methods in Ecology and Evolution*, *10*(11), 1941–1951. https://doi.org/10.1111/2041-210X.13289

Beirne, C., Waring, L., McDonald, R. A., Delahay, R., & Young, A. (2016). Age-related declines in immune response in a wild mammal are unrelated to immune cell telomere length. *Proceedings of the Royal Society B: Biological Sciences*, *283*(1825), 20152949. https://doi.org/10.1098/rspb.2015.2949

Bichet, C., Bouwhuis, S., Bauch, C., Verhulst, S., Becker, P. H., & Vedder, O. (2020). Telomere length is repeatable, shortens with age and reproductive success, and predicts remaining lifespan in a long-lived seabird. *Molecular Ecology*, *29*(2), 429–441. https://doi.org/10.1111/mec.15331

Bichet, C., Moiron, M., Kürten, N., Vedder, O., & Bouwhuis, S. (2025). Egg Characteristics of Female Common Terns Are Repeatable, and Vary With Maternal Age and Laying Order. *Ecology and Evolution*, *15*(11), e72455. https://doi.org/10.1002/ece3.72455

Bichet, C., Moiron, M., Matson, K. D., Vedder, O., & Bouwhuis, S. (2022). Immunosenescence in the wild? A longitudinal study in a long-lived seabird. *Journal of Animal Ecology*, *91*(2), 458–469. https://doi.org/10.1111/1365-2656.13642

Bouwhuis, S., Charmantier, A., Verhulst, S., & Sheldon, B. C. (2010a). Individual variation in rates of senescence: Natal origin effects and disposable soma in a wild bird population. *Journal of Animal Ecology*, *79*(6), 1251–1261. https://doi.org/10.1111/j.1365-2656.2010.01730.x

Bouwhuis, S., Charmantier, A., Verhulst, S., & Sheldon, B. C. (2010b). Trans-generational effects on ageing in a wild bird population. *Journal of Evolutionary Biology*, *23*(3), 636–642. https://doi.org/10.1111/j.1420-9101.2009.01929.x

Bouwhuis, S., Choquet, R., Sheldon, B. C., & Verhulst, S. (2012). The Forms and Fitness Cost of Senescence: Age-Specific Recapture, Survival, Reproduction, and Reproductive Value in a Wild Bird Population. *The American Naturalist*, *179*(1), E15–E27. https://doi.org/10.1086/663194

Bouwhuis, S., Sheldon, B. C., Verhulst, S., & Charmantier, A. (2009). Great tits growing old: Selective disappearance and the partitioning of senescence to stages within the breeding cycle. *Proceedings of the Royal Society B: Biological Sciences*, *276*(1668), 2769–2777. https://doi.org/10.1098/rspb.2009.0457

Bouwhuis, S., & Vedder, O. (2017). Avian Escape Artists?: Patterns, Processes and Costs of Senescence in Wild Birds. In R. P. Shefferson, O. R. Jones, & R. Salguero-Gómez (Eds.), *The Evolution of Senescence in the Tree of Life* (1st ed., pp. 156–174). Cambridge University Press. https://doi.org/10.1017/9781139939867.008

Bouwhuis, S., Vedder, O., & Becker, P. H. (2015). Sex-specific pathways of parental age effects on offspring lifetime reproductive success in a long-lived seabird: SEX-SPECIFIC PARENTAL EFFECTS ON OFFSPRING FITNESS. *Evolution*, *69*(7), 1760–1771. https://doi.org/10.1111/evo.12692

Brooks, R., & Kemp, D. J. (2001). Can older males deliver the good genes? *Trends in Ecology & Evolution*, *16*(6), 308–313. https://doi.org/10.1016/S0169-5347(01)02147-4

Cam, E., Link, W. A., Cooch, E. G., Monnat, J., & Danchin, E. (2002). Individual Covariation in Life-History Traits: Seeing the Trees Despite the Forest. *The American Naturalist*, *159*(1), 96–105. https://doi.org/10.1086/324126

Cam, E., & Monnat, J. Y. (2000). Stratification based on reproductive state reveals contrasting patterns of age-related variation in demographic parameters in the kittiwake. *Oikos*, *90*(3), 560–574. https://doi.org/10.1034/j.1600-0706.2000.900314.x

Cansse, T., Vedder, O., Kürten, N., & Bouwhuis, S. (2024). Feeding rate reflects quality in both parents and offspring: A longitudinal study in common terns. *Animal Behaviour*, *214*, 111–120. https://doi.org/10.1016/j.anbehav.2024.06.010

Chen, H., Jolly, C., Bublys, K., Marcu, D., & Immler, S. (2020). Trade-off between somatic and germline repair in a vertebrate supports the expensive germ line hypothesis. *Proceedings of the National Academy of Sciences*, *117*(16), 8973–8979. https://doi.org/10.1073/pnas.1918205117

Cooper, E. B., Bonnet, T., Osmond, H. L., Cockburn, A., & Kruuk, L. E. B. (2021). Aging and Senescence across Reproductive Traits and Survival in Superb Fairy-Wrens (*Malurus cyaneus*). *The American Naturalist*, *197*(1), 111–127. https://doi.org/10.1086/711755

Cope, H., Ivimey-Cook, E. R., & Moorad, J. (2022). Triparental ageing in a laboratory population of an insect with maternal care. *Behavioral Ecology*, *33*(6), 1123–1132. https://doi.org/10.1093/beheco/arac078

Donertas, H. M., & Partridge, L. (2025). The Evolution of Human Ageing Under the Shadow of Demographic Transition. *bioRxiv*. https://doi.org/10.64898/2025.12.03.691940; t

Duffield, K. R., Bowers, E. K., Sakaluk, S. K., & Sadd, B. M. (2017). A dynamic threshold model for terminal investment. *Behavioral Ecology and Sociobiology*, *71*(12), 185. https://doi.org/10.1007/s00265-017-2416-z

Dugdale, H. L., Pope, L. C., Newman, C., Macdonald, D. W., & Burke, T. (2011). Age-specific breeding success in a wild mammalian population: Selection, constraint, restraint and senescence: AGE-SPECIFIC BREEDING SUCCESS IN BADGERS. *Molecular Ecology*, *20*(15), 3261–3274. https://doi.org/10.1111/j.1365-294X.2011.05167.x

Evans, S. R., Gustafsson, L., & Sheldon, B. C. (2011). DIVERGENT PATTERNS OF AGE-DEPENDENCE IN ORNAMENTAL AND REPRODUCTIVE TRAITS IN THE COLLARED FLYCATCHER: AGING OF ORNAMENTS AND REPRODUCTIVE TRAITS. *Evolution*, *65*(6), 1623–1636. https://doi.org/10.1111/j.1558-5646.2011.01253.x

Fay, R., Barbraud, C., Delord, K., & Weimerskirch, H. (2018). From early life to senescence: Individual heterogeneity in a long-lived seabird. *Ecological Monographs*, *88*(1), 60–73. https://doi.org/10.1002/ecm.1275

Fay, R., Martin, J., & Plard, F. (2022). Distinguishing within- from between-individual effects: How to use the within-individual centring method for quadratic patterns. *Journal of Animal Ecology*, *91*(1), 8–19. https://doi.org/10.1111/1365-2656.13606

Fay, R., Ravussin, P.-A., Arrigo, D., Von Rönn, J. A. C., & Schaub, M. (2021). Age-specific reproduction in female pied flycatchers: Evidence for asynchronous aging. *Oecologia*, *196*(3), 723–734. https://doi.org/10.1007/s00442-021-04963-2

Forslund, P., & Pärt, T. (1995). Age and reproduction in birds—Hypotheses and tests. *Trends in Ecology & Evolution*, *10*(9), 374–378. https://doi.org/10.1016/S0169-5347(00)89141-7

Froy, H., Phillips, R. A., Wood, A. G., Nussey, D. H., & Lewis, S. (2013). Age-related variation in reproductive traits in the wandering albatross: Evidence for terminal improvement following senescence. *Ecology Letters*, *16*(5), 642–649. https://doi.org/10.1111/ele.12092

Gaillard, J., & Lemaître, J. (2020). An integrative view of senescence in nature. *Functional Ecology*, *34*(1), 4–16. https://doi.org/10.1111/1365-2435.13506

González-Bernardo, E., Martínez-Padilla, J., Camacho, C., García Del Castillo, M. E., Potti, J., & Canal, D. (2025). Sex- and trait-specific contribution of individual- and population-level processes to age-related changes in multiple plumage ornaments. *iScience*, *28*(5), 112512. https://doi.org/10.1016/j.isci.2025.112512

Hämäläinen, A., Dammhahn, M., Aujard, F., Eberle, M., Hardy, I., Kappeler, P. M., Perret, M., Schliehe-Diecks, S., & Kraus, C. (2014). Senescence or selective disappearance? Age trajectories of body mass in wild and captive populations of a small-bodied primate. *Proceedings of the Royal Society B: Biological Sciences*, *281*(1791), 20140830. https://doi.org/10.1098/rspb.2014.0830

Hamel, S., Gaillard, J., Douhard, M., Festa-Bianchet, M., Pelletier, F., & Yoccoz, N. G. (2018). Quantifying individual heterogeneity and its influence on life-history trajectories: Different methods for different questions and contexts. *Oikos*, *127*(5), 687–704. https://doi.org/10.1111/oik.04725

Hamilton, W. D. (1966). The moulding of senescence by natural selection. *Journal of Theoretical Biology*, *12*(1), 12–45. https://doi.org/10.1016/0022-5193(66)90184-6

Hansen, T. F., & Price, D. K. (1995). Good genes and old age: Do old mates provide superior genes? *Journal of Evolutionary Biology*, *8*(6), 759–778. https://doi.org/10.1046/j.1420-9101.1995.8060759.x

Haussmann, M. F., & Mauck, R. A. (2007). Telomeres and Longevity: Testing an Evolutionary Hypothesis. *Molecular Biology and Evolution*, *25*(1), 220–228. https://doi.org/10.1093/molbev/msm244

Hayward, A. D., Wilson, A. J., Pilkington, J. G., Clutton-Brock, T. H., Pemberton, J. M., & Kruuk, L. E. B. (2013). Reproductive senescence in female S oay sheep: Variation across traits and contributions of individual ageing and selective disappearance. *Functional Ecology*, *27*(1), 184–195. https://doi.org/10.1111/1365-2435.12029

Healy, K., Ezard, T. H. G., Jones, O. R., Salguero-Gómez, R., & Buckley, Y. M. (2019). Animal life history is shaped by the pace of life and the distribution of age-specific mortality and reproduction. *Nature Ecology & Evolution*, *3*(8), 1217–1224. https://doi.org/10.1038/s41559-019-0938-7

Ivimey-Cook, E., & Moorad, J. (2018). Disentangling Pre- and Postnatal Maternal Age Effects on Offspring Performance in an Insect with Elaborate Maternal Care. *The American Naturalist*, *192*(5), 564–576. https://doi.org/10.1086/699654

Janeiro, M. J., Henshaw, J. M., Pemberton, J. M., Pilkington, J. G., & Morrissey, M. B. (2025). An early-life survival and reproductive trade-off shapes selection on body size. *Evolution Letters*, qraf029. https://doi.org/10.1093/evlett/qraf029

Johnson, S. L., & Gemmell, N. J. (2012). Are old males still good males and can females tell the difference?: Do hidden advantages of mating with old males off-set costs related to fertility, or are we missing something else? *BioEssays*, *34*(7), 609–619. https://doi.org/10.1002/bies.201100157

Johnson, S. L., Zellhuber-McMillan, S., Gillum, J., Dunleavy, J., Evans, J. P., Nakagawa, S., & Gemmell, N. J. (2018). Evidence that fertility trades off with early offspring fitness as males age. *Proceedings of the Royal Society B: Biological Sciences*, *285*(1871), 20172174. https://doi.org/10.1098/rspb.2017.2174

Jones, O. R., Scheuerlein, A., Salguero-Gómez, R., Camarda, C. G., Schaible, R., Casper, B. B., Dahlgren, J. P., Ehrlén, J., García, M. B., Menges, E. S., Quintana-Ascencio, P. F., Caswell, H., Baudisch, A., & Vaupel, J. W. (2014). Diversity of ageing across the tree of life. *Nature*, *505*(7482), 169–173. https://doi.org/10.1038/nature12789

Kauzálová, T., Tomášek, O., Mulder, E., Verhulst, S., & Albrecht, T. (2022). Telomere length is highly repeatable and shorter in individuals with more elaborate sexual ornamentation in a short-lived passerine. *Molecular Ecology*, *31*(23), 6172–6183. https://doi.org/10.1111/mec.16397

Kervinen, M., Lebigre, C., Alatalo, R. V., Siitari, H., & Soulsbury, C. D. (2015). Life-History Differences in Age-Dependent Expressions of Multiple Ornaments and Behaviors in a Lekking Bird. *The American Naturalist*, *185*(1), 13–27. https://doi.org/10.1086/679012

Kirkwood, T. B. L., & Rose, M. R. (1991). Evolution of senescence: Late survival sacrificed for reproduction. *Philosophical Transactions of the Royal Society of London. Series B: Biological Sciences*, *332*(1262), 15–24. https://doi.org/10.1098/rstb.1991.0028

Kokko, H. (1998). Good genes, old age and life-history trade-offs. *Evolutionary Ecology*, *12*(6), 739–750. https://doi.org/10.1023/A:1006541701002

Lailvaux, S. P., & Kasumovic, M. M. (2011). Defining individual quality over lifetimes and selective contexts. *Proceedings of the Royal Society B: Biological Sciences*, *278*(1704), 321–328. https://doi.org/10.1098/rspb.2010.1591

Lemaître, J.-F., Berger, V., Bonenfant, C., Douhard, M., Gamelon, M., Plard, F., & Gaillard, J.-M. (2015). Early-late life trade-offs and the evolution of ageing in the wild. *Proceedings of the Royal Society B: Biological Sciences*, *282*(1806), 20150209. https://doi.org/10.1098/rspb.2015.0209

Lemaître, J.-F., & Gaillard, J.-M. (2017). Reproductive senescence: New perspectives in the wild: Reproductive senescence in the wild. *Biological Reviews*, *92*(4), 2182–2199. https://doi.org/10.1111/brv.12328

Lemaître, J.-F., Moorad, J., Gaillard, J.-M., Maklakov, A. A., & Nussey, D. H. (2024). A unified framework for evolutionary genetic and physiological theories of aging. *PLOS Biology*, *22*(2), e3002513. https://doi.org/10.1371/journal.pbio.3002513

Lemaître, J.-F., Ronget, V., & Gaillard, J.-M. (2020). Female reproductive senescence across mammals: A high diversity of patterns modulated by life history and mating traits. *Mechanisms of Ageing and Development*, *192*, 111377. https://doi.org/10.1016/j.mad.2020.111377

Lopez-Idiaquez, D., Vergara, P., Fargallo, J. A., & Martinez-Padilla, J. (2016). Old males reduce melanin-pigmented traits and increase reproductive outcome under worse environmental conditions in common kestrels. *Ecology and Evolution*, *6*(4), 1224–1235. https://doi.org/10.1002/ece3.1910

Maklakov, A. A., Carlsson, H., Denbaum, P., Lind, M. I., Mautz, B., Hinas, A., & Immler, S. (2017). Antagonistically pleiotropic allele increases lifespan and late-life reproduction at the cost of early-life reproduction and individual fitness. *Proceedings of the Royal Society B: Biological Sciences*, *284*(1856), 20170376. https://doi.org/10.1098/rspb.2017.0376

Maklakov, A. A., & Chapman, T. (2019). Evolution of ageing as a tangle of trade-offs: Energy versus function. *Proceedings of the Royal Society B: Biological Sciences*, *286*(1911), 20191604. https://doi.org/10.1098/rspb.2019.1604

Maklakov, A. A., Rowe, L., & Friberg, U. (2015). Why organisms age: Evolution of senescence under positive pleiotropy? *BioEssays*, *37*(7), 802–807. https://doi.org/10.1002/bies.201500025

Marcu, D., Cohen-Krais, J., Godden, A., Alavioon, G., Martins, C., Almstrup, K., Saalbach, G., & Immler, S. (2024). *Within-ejaculate haploid selection reduces disease biomarkers in human sperm*. https://doi.org/10.1101/2024.10.08.617222

Martinig, A. R., Mathot, K. J., Lane, J. E., Dantzer, B., & Boutin, S. (2021). Selective disappearance does not underlie age-related changes in trait repeatability in red squirrels. *Behavioral Ecology*, *32*(2), 306–315. https://doi.org/10.1093/beheco/araa136

McCleery, R. H., Perrins, C. M., Sheldon, B. C., & Charmantier, A. (2008). Age-specific reproduction in a long-lived species: The combined effects of senescence and individual quality. *Proceedings of the Royal Society B: Biological Sciences*, *275*(1637), 963–970. https://doi.org/10.1098/rspb.2007.1418

McLean, E. M., Archie, E. A., & Alberts, S. C. (2019). Lifetime Fitness in Wild Female Baboons: Trade-Offs and Individual Heterogeneity in Quality. *The American Naturalist*, *194*(6), 745–759. https://doi.org/10.1086/705810

Mittell, E. A., Pemberton, J. M., Kruuk, L. E. B., & Morrissey, M. B. (2025). Unmeasured prior viability selection resolves the paradox of stasis for body size in wild Soay sheep. *Proceedings of the National Academy of Sciences*, *122*(48), e2513969122. https://doi.org/10.1073/pnas.2513969122

Moiron, M., & Bouwhuis, S. (2024). Age-dependent shaping of the social environment in a long-lived seabird: A quantitative genetic approach. *Philosophical Transactions of the Royal Society B: Biological Sciences*, *379*(1916), 20220465. https://doi.org/10.1098/rstb.2022.0465

Moullec, H., Berger, V., Meier, C., Reichert, S., & Bize, P. (2025). Effects of parental age at conception on offspring life history trajectories in a long-lived bird. *Evolution*, qpaf181. https://doi.org/10.1093/evolut/qpaf181

Murgatroyd, M., Roos, S., Evans, R., Sansom, A., Whitfield, D. P., Sexton, D., Reid, R., Grant, J., & Amar, A. (2018). Sex-specific patterns of reproductive senescence in a long-lived reintroduced raptor. *Journal of Animal Ecology*, *87*(6), 1587–1599. https://doi.org/10.1111/1365-2656.12880

Nussey, D. H., Coulson, T., Delorme, D., Clutton-Brock, T. H., Pemberton, J. M., Festa-Bianchet, M., & Gaillard, J.-M. (2011). Patterns of body mass senescence and selective disappearance differ among three species of free-living ungulates. *Ecology*, *92*(10), 1936–1947. https://doi.org/10.1890/11-0308.1

Nussey, D. H., Coulson, T., Festa-Bianchet, M., & Gaillard, J. -M. (2008). Measuring senescence in wild animal populations: Towards a longitudinal approach. *Functional Ecology*, *22*(3), 393–406. https://doi.org/10.1111/j.1365-2435.2008.01408.x

Nussey, D. H., Froy, H., Lemaitre, J.-F., Gaillard, J.-M., & Austad, S. N. (2013). Senescence in natural populations of animals: Widespread evidence and its implications for bio-gerontology. *Ageing Research Reviews*, *12*(1), 214–225. https://doi.org/10.1016/j.arr.2012.07.004

Nussey, D. H., Kruuk, L. E. B., Donald, A., Fowlie, M., & Clutton-Brock, T. H. (2006). The rate of senescence in maternal performance increases with early-life fecundity in red deer. *Ecology Letters*, *9*(12), 1342–1350. https://doi.org/10.1111/j.1461-0248.2006.00989.x

Nussey, D. H., Kruuk, L. E. B., Morris, A., Clements, M. N., Pemberton, J. M., & Clutton-Brock, T. H. (2009). Inter- and Intrasexual Variation in Aging Patterns across Reproductive Traits in a Wild Red Deer Population. *The American Naturalist*, *174*(3), 342–357. https://doi.org/10.1086/603615

Pepke, M. L., Kvalnes, T., Wright, J., Araya-Ajoy, Y. G., Ranke, P. S., Boner, W., Monaghan, P., Sæther, B.-E., Jensen, H., & Ringsby, T. H. (2023). Longitudinal telomere dynamics within natural lifespans of a wild bird. *Scientific Reports*, *13*(1), 4272. https://doi.org/10.1038/s41598-023-31435-9

Peters, A., Delhey, K., Nakagawa, S., Aulsebrook, A., & Verhulst, S. (2019). Immunosenescence in wild animals: Meta-analysis and outlook. *Ecology Letters*, *22*(10), 1709–1722. https://doi.org/10.1111/ele.13343

Power, M. L., Ransome, R. D., Riquier, S., Romaine, L., Jones, G., & Teeling, E. C. (2023). Hibernation telomere dynamics in a shifting climate: Insights from wild greater horseshoe bats. *Proceedings of the Royal Society B: Biological Sciences*, *290*(2008), 20231589. https://doi.org/10.1098/rspb.2023.1589

Power, M. L., Ransome, R. D., Romaine, L., Jones, G., & Teeling, E. C. (2025). Short- and long-term costs of reproduction revealed by telomere dynamics in wild greater horseshoe bats. *Proceedings of the National Academy of Sciences*, *122*(50), e2515125122. https://doi.org/10.1073/pnas.2515125122

Réale, D., Garant, D., Humphries, M. M., Bergeron, P., Careau, V., & Montiglio, P.-O. (2010). Personality and the emergence of the pace-of-life syndrome concept at the population level. *Philosophical Transactions of the Royal Society B: Biological Sciences*, *365*(1560), 4051–4063. https://doi.org/10.1098/rstb.2010.0208

Rebke, M., Coulson, T., Becker, P. H., & Vaupel, J. W. (2010). Reproductive improvement and senescence in a long-lived bird. *Proceedings of the National Academy of Sciences*, *107*(17), 7841–7846. https://doi.org/10.1073/pnas.1002645107

Reed, T. E., Kruuk, L. E. B., Wanless, S., Frederiksen, M., Cunningham, E. J. A., & Harris, M. P. (2008). Reproductive Senescence in a Long-Lived Seabird: Rates of Decline in Late-Life Performance Are Associated with Varying Costs of Early Reproduction. *The American Naturalist*, *171*(2), E89–E101. https://doi.org/10.1086/524957

Reid, J. M., Bignal, E. M., Bignal, S., McCracken, D. I., & Monaghan, P. (2003). Age-specific reproductive performance in red-billed choughs *Pyrrhocorax pyrrhocorax*: Patterns and processes in a natural population. *Journal of Animal Ecology*, *72*(5), 765–776. https://doi.org/10.1046/j.1365-2656.2003.00750.x

Reznick, D., Nunney, L., & Tessier, A. (2000). Big houses, big cars, superfleas and the costs of reproduction. *Trends in Ecology & Evolution*, *15*(10), 421–425. https://doi.org/10.1016/S0169-5347(00)01941-8

Robinson, M. R., Mar, K. U., & Lummaa, V. (2012). Senescence and age-specific trade-offs between reproduction and survival in female Asian elephants. *Ecology Letters*, *15*(3), 260–266. https://doi.org/10.1111/j.1461-0248.2011.01735.x

Roff, D. A., & Fairbairn, D. J. (2007). The evolution of trade-offs: Where are we? *Journal of Evolutionary Biology*, *20*(2), 433–447. https://doi.org/10.1111/j.1420-9101.2006.01255.x

Sadoughi, B., Mundry, R., Schülke, O., & Ostner, J. (2024). Social network shrinking is explained by active and passive effects but not increasing selectivity with age in wild macaques. *Proceedings of the Royal Society B: Biological Sciences*, *291*(2018), 20232736. https://doi.org/10.1098/rspb.2023.2736

997 Salmón, P., Nilsson, J. F., Watson, H., Bensch, S., & Isaksson, C. (2017). Selective disappearance of great tits
998 with short telomeres in urban areas. *Proceedings of the Royal Society B: Biological Sciences*, *284*(1862),
999 20171349. https://doi.org/10.1098/rspb.2017.1349

1000 Sanghvi, K., Zajitschek, F., Iglesias-Carrasco, M., & Head, M. L. (2021). Sex- and trait-specific silver-spoon
1001 effects of developmental environments, on ageing. *Evolutionary Ecology*, *35*(3), 367–385.
1002 https://doi.org/10.1007/s10682-021-10115-y

1003 Sanghvi, K., Vega-Trejo, R., Nakagawa, S., Gascoigne, S. J. L., Johnson, S. L., Salguero-Gómez, R., Pizzari, T.,
1004 & Sepil, I. (2024a). Meta-analysis shows no consistent evidence for senescence in ejaculate traits across
1005 animals. *Nature Communications*, *15*(1), 558. https://doi.org/10.1038/s41467-024-44768-4

1006 Sanghvi, K., Pizzari, T., & Sepil, I. (2024b). What doesn't kill you makes you stronger? Effects of paternal age
1007 at conception on fathers and sons. *Evolution*, qpae097. https://doi.org/10.1093/evolut/qpae097

1008 Sanghvi, K., Iglesias-Carrasco, M., Zajitschek, F., Kruuk, L. E. B., & Head, M. L. (2022). Effects of
1009 developmental and adult environments on ageing. *Evolution*, *76*(8), 1868–1882.
1010 https://doi.org/10.1111/evo.14567

1011 Sanghvi, K., Gascoigne, S. J. L., & Sepil, I. (2025a). *Mechanisms of phenotypic trade-offs in the resource*
1012 *acquisition-allocation Y-model*. Cold Spring Harbor Laboratory. https://doi.org/10.1101/2025.07.07.662185

1013 Sanghvi, K., Gascoigne, S. J. L., Todorova, B., Vega-Trejo, R., Pizzari, T., & Sepil, I. (2025b). No evidence for
1014 paternal age effects on sons or daughters, when accounting for paternal sperm storage. *The American Naturalist*,
1015 736479. https://doi.org/10.1086/736479

1016 Sanghvi, K., Dean, R., Nakagawa, S., Reinhardt, K., Sepil, I., & Vega-Trejo, R. (2025c). *Sperm storage reduces*
1017 *sperm and embryo quality in animals*. https://doi.org/10.1101/2025.04.10.647966

1018 Sanghvi, K., Shandilya, S., Brown, A., Todorova, B., Jahn, M., Gascoigne, S. J. L., Camilleri, T.-L., Pizzari, T.,
1019 & Sepil, I. (2025d). Reproductive output of old males is limited by seminal fluid, not sperm number. *Evolution*
1020 *Letters*, qrae071. https://doi.org/10.1093/evlett/qrae071

1021 Sanghvi, K., Henshaw, J. M., Kacelnik, A., Janicke, T., & Sepil, I. (2025e). Diagnosing confounded Bateman
1022 gradients. *Evolution*, qpaf127. https://doi.org/10.1093/evolut/qpaf127

1023 Sergio, F., Tanferna, A., De Stephanis, R., Jiménez, L. L., Blas, J., Tavecchia, G., Preatoni, D., & Hiraldo, F.
1024 (2014). Individual improvements and selective mortality shape lifelong migratory performance. *Nature*,
1025 *515*(7527), 410–413. https://doi.org/10.1038/nature13696

1026 Sharp, S. P., & Clutton-Brock, T. H. (2010). Reproductive senescence in a cooperatively breeding mammal.
1027 *Journal of Animal Ecology*, *79*(1), 176–183. https://doi.org/10.1111/j.1365-2656.2009.01616.x

1028 Simons, M. J. P., Briga, M., & Verhulst, S. (2016). Stabilizing survival selection on presenescent expression of a
1029 sexual ornament followed by a terminal decline. *Journal of Evolutionary Biology*, *29*(7), 1368–1378.
1030 https://doi.org/10.1111/jeb.12877

1031 Siracusa, E. R., Negron-Del Valle, J. E., Phillips, D., Platt, M. L., Higham, J. P., Snyder-Mackler, N., & Brent,
1032 L. J. N. (2022). Within-individual changes reveal increasing social selectivity with age in rhesus macaques.
1033 *Proceedings of the National Academy of Sciences*, *119*(49), e2209180119.
1034 https://doi.org/10.1073/pnas.2209180119

1035 Smallegange, I. M., & Guenther, A. (2025). A development-centric perspective on pace-of-life syndromes.
1036 *Evolution Letters*, *9*(2), 172–183. https://doi.org/10.1093/evlett/qrae069

1037 Spagopoulou, F., Teplitsky, C., Chantepie, S., Lind, M. I., Gustafsson, L., & Maklakov, A. A. (2020). Silver-
1038 spoon upbringing improves early-life fitness but promotes reproductive ageing in a wild bird. *Ecology Letters*,
1039 *23*(6), 994–1002. https://doi.org/10.1111/ele.13501

1040 Sparks, A. M., Hammers, M., Komdeur, J., Burke, T., Richardson, D. S., & Dugdale, H. L. (2022). Sex-
1041 dependent effects of parental age on offspring fitness in a cooperatively breeding bird. *Evolution Letters*, *6*(6),
1042 438–449. https://doi.org/10.1002/evl3.300

Sun, Y., Burke, T. A., Dugdale, H. L., & Schroeder, J. (2025). Long-term fitness effects of the early-life environment in a wild bird population. *Behavioral Ecology*, *36*(5), araf097. https://doi.org/10.1093/beheco/araf097

Tarwater, C. E., & Arcese, P. (2017). Age and years to death disparately influence reproductive allocation in a short-lived bird. *Ecology*, *98*(9), 2248–2254. https://doi.org/10.1002/ecy.1851

Thorley, J., Duncan, C., Sharp, S. P., Gaynor, D., Manser, M. B., & Clutton-Brock, T. (2020). Sex-independent senescence in a cooperatively breeding mammal. *Journal of Animal Ecology*, *89*(4), 1080–1093. https://doi.org/10.1111/1365-2656.13173

Torres, R., Drummond, H., & Velando, A. (2011). Parental Age and Lifespan Influence Offspring Recruitment: A Long-Term Study in a Seabird. *PLoS ONE*, *6*(11), e27245. https://doi.org/10.1371/journal.pone.0027245

Tuljapurkar, S., Steiner, U. K., & Orzack, S. H. (2009). Dynamic heterogeneity in life histories. *Ecology Letters*, *12*(1), 93–106. https://doi.org/10.1111/j.1461-0248.2008.01262.x

Van De Pol, M., & Verhulst, S. (2006). Age-Dependent Traits: A New Statistical Model to Separate Within- and Between-Individual Effects. *The American Naturalist*, *167*(5), 766–773. https://doi.org/10.1086/503331

Van De Pol, M., & Wright, J. (2009). A simple method for distinguishing within- versus between-subject effects using mixed models. *Animal Behaviour*, *77*(3), 753–758. https://doi.org/10.1016/j.anbehav.2008.11.006

Van De Walle, J., Fay, R., Gaillard, J.-M., Pelletier, F., Hamel, S., Gamelon, M., Barbraud, C., Blanchet, F. G., Blumstein, D. T., Charmantier, A., Delord, K., Larue, B., Martin, J., Mills, J. A., Milot, E., Mayer, F. M., Rotella, J., Saether, B.-E., Teplitsky, C., … Jenouvrier, S. (2023). Individual life histories: Neither slow nor fast, just diverse. *Proceedings of the Royal Society B: Biological Sciences*, *290*(2002), 20230511. https://doi.org/10.1098/rspb.2023.0511

Van Noordwijk, A. J., & De Jong, G. (1986). Acquisition and Allocation of Resources: Their Influence on Variation in Life History Tactics. *The American Naturalist*, *128*(1), 137–142. https://doi.org/10.1086/284547

Vaupel, J. W., Manton, K. G., & Stallard, E. (1979). The impact of heterogeneity in individual frailty on the dynamics of mortality. *Demography*, *16*(3), 439–454. https://doi.org/10.2307/2061224

Vaupel, J. W., & Yashin, A. I. (1985). Heterogeneity's Ruses: Some Surprising Effects of Selection on Population Dynamics. *The American Statistician*, *39*(3), 176–185. https://doi.org/10.1080/00031305.1985.10479424

Vindenes, Y., Engen, S., & Sæther, B. (2008). Individual Heterogeneity in Vital Parameters and Demographic Stochasticity. *The American Naturalist*, *171*(4), 455–467. https://doi.org/10.1086/528965

Westneat, D. F., Araya-Ajoy, Y. G., Allegue, H., Class, B., Dingemanse, N., Dochtermann, N. A., Garamszegi, L. Z., Martin, J. G. A., Nakagawa, S., Réale, D., & Schielzeth, H. (2020). Collision between biological process and statistical analysis revealed by mean centring. *Journal of Animal Ecology*, *89*(12), 2813–2824. https://doi.org/10.1111/1365-2656.13360

Williams, G. C. (1957). Pleiotropy, Natural Selection, and the Evolution of Senescence. *Evolution*, *11*(4), 398. https://doi.org/10.2307/2406060

Williams, P. D., & Day, T. (2003). ANTAGONISTIC PLEIOTROPY, MORTALITY SOURCE INTERACTIONS, AND THE EVOLUTIONARY THEORY OF SENESCENCE. *Evolution*, *57*(7), 1478–1488. https://doi.org/10.1111/j.0014-3820.2003.tb00356.x

Wilson, A. J., & Nussey, D. H. (2010). What is individual quality? An evolutionary perspective. *Trends in Ecology & Evolution*, *25*(4), 207–214. https://doi.org/10.1016/j.tree.2009.10.002

Winter, B., & Wieling, M. (2016). How to analyze linguistic change using mixed models, Growth Curve Analysis and Generalized Additive Modeling. *Journal of Language Evolution*, *1*(1), 7–18. https://doi.org/10.1093/jole/lzv003

Wynn, J., Kürten, N., Moiron, M., & Bouwhuis, S. (2025). Selective disappearance based on navigational efficiency in a long-lived seabird. *Journal of Animal Ecology*, *94*(4), 535–544. https://doi.org/10.1111/1365-2656.14231

Zhang, H., Vedder, O., Becker, P. H., & Bouwhuis, S. (2015). Age-dependent trait variation: The relative contribution of within-individual change, selective appearance and disappearance in a long-lived seabird. *Journal of Animal Ecology*, *84*(3), 797–807. https://doi.org/10.1111/1365-2656.12321

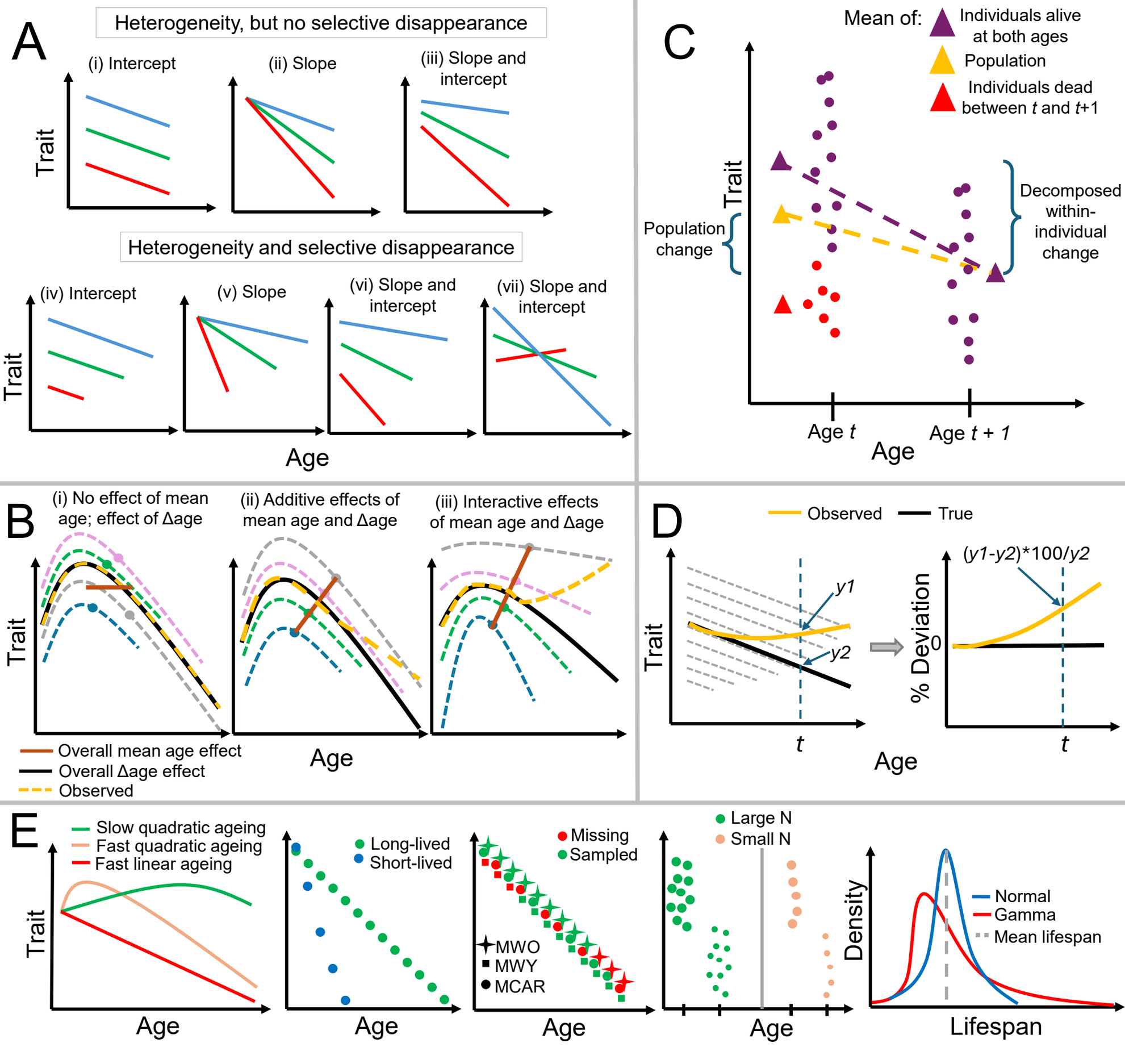
A
Heterogeneity, but no selective disappearance
(i) Intercept
(ii) Slope
(iii) Slope and intercept
Trait
Heterogeneity and selective disappearance
(iv) Intercept
(v) Slope
(vi) Slope and intercept
(vii) Slope and intercept
Trait
Age
C
Mean of:
Individuals alive at both ages
Population
Individuals dead between t and t+1
Trait
Population change
Decomposed within-individual change
Age t
Age t + 1
Age
B
(i) No effect of mean age; effect of Δage
(ii) Additive effects of mean age and Δage
(iii) Interactive effects of mean age and Δage
Trait
Overall mean age effect
Overall Δage effect
Observed
Age
D
Observed
True
Trait
y1
y2
t
(y1-y2)*100/y2
% Deviation
0
t
Age
E
Slow quadratic ageing
Fast quadratic ageing
Fast linear ageing
Trait
Age
Long-lived
Short-lived
Age
Missing
Sampled
MWO
MWY
MCAR
Age
Large N
Small N
Age
Density
Normal
Gamma
Mean lifespan
Lifespan

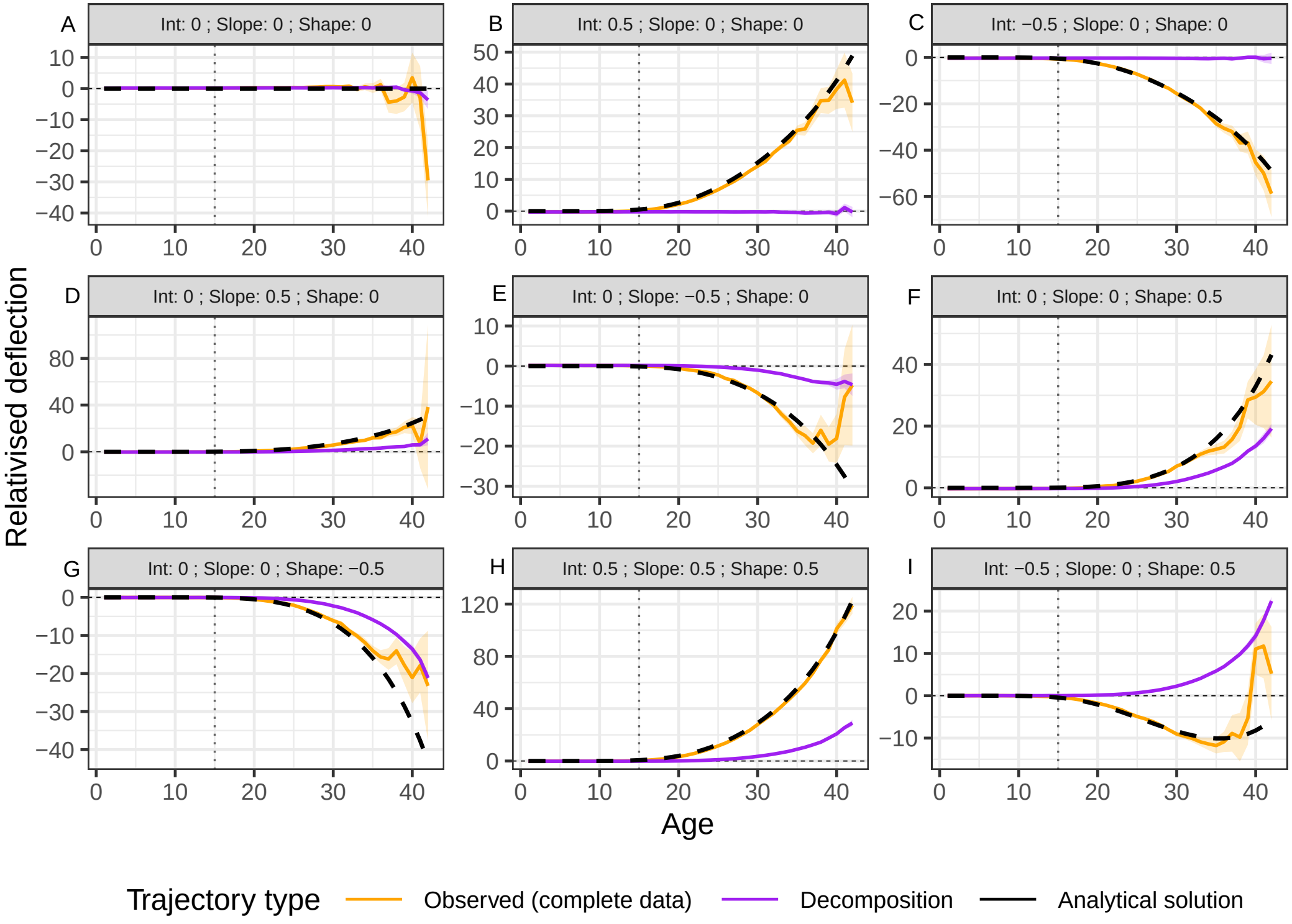
A
Int: 0 ; Slope: 0 ; Shape: 0
B
Int: 0.5 ; Slope: 0 ; Shape: 0
C
Int: −0.5 ; Slope: 0 ; Shape: 0
D
Int: 0 ; Slope: 0.5 ; Shape: 0
E
Int: 0 ; Slope: −0.5 ; Shape: 0
F
Int: 0 ; Slope: 0 ; Shape: 0.5
G
Int: 0 ; Slope: 0 ; Shape: −0.5
H
Int: 0.5 ; Slope: 0.5 ; Shape: 0.5
I
Int: −0.5 ; Slope: 0 ; Shape: 0.5
Relativised deflection
Age
Trajectory type
Observed (complete data)
Decomposition
Analytical solution

A
Int: 0 ; Slope: 0 ; Shape: 0
B
Int: 0.5 ; Slope: 0 ; Shape: 0
C
Int: −0.5 ; Slope: 0 ; Shape: 0
D
Int: 0 ; Slope: 0.5 ; Shape: 0
E
Int: 0 ; Slope: −0.5 ; Shape: 0
F
Int: 0 ; Slope: 0 ; Shape: 0.5
G
Int: 0 ; Slope: 0 ; Shape: −0.5
H
Int: 0.5 ; Slope: 0.5 ; Shape: 0.5
I
Int: −0.5 ; Slope: −0.5 ; Shape: −0.5
ΔAIC
200
100
0
−100
300
200
100
0
−100
300
200
100
0
−100
500
250
0
500
250
0
500
250
0
500
250
0
2000
1000
0
2000
1000
0
Model 1
Model 2
Model 3
Model 4
Model 5
Model

A
Int: 0 ; Slope: 0 ; Shape: 0
B
Int: 0.5 ; Slope: 0 ; Shape: 0
C
Int: −0.5 ; Slope: 0 ; Shape: 0
D
Int: 0 ; Slope: 0.5 ; Shape: 0
E
Int: 0 ; Slope: −0.5 ; Shape: 0
F
Int: 0 ; Slope: 0 ; Shape: 0.5
G
Int: 0 ; Slope: 0 ; Shape: −0.5
H
Int: 0.5 ; Slope: 0.5 ; Shape: 0.5
I
Int: −0.5 ; Slope: −0.5 ; Shape: −0.5
Deflection of model/method prediction from True
Age
Method or Model
Decomposition
Model 1
Model 2
Model 3
Model 4
Model 5

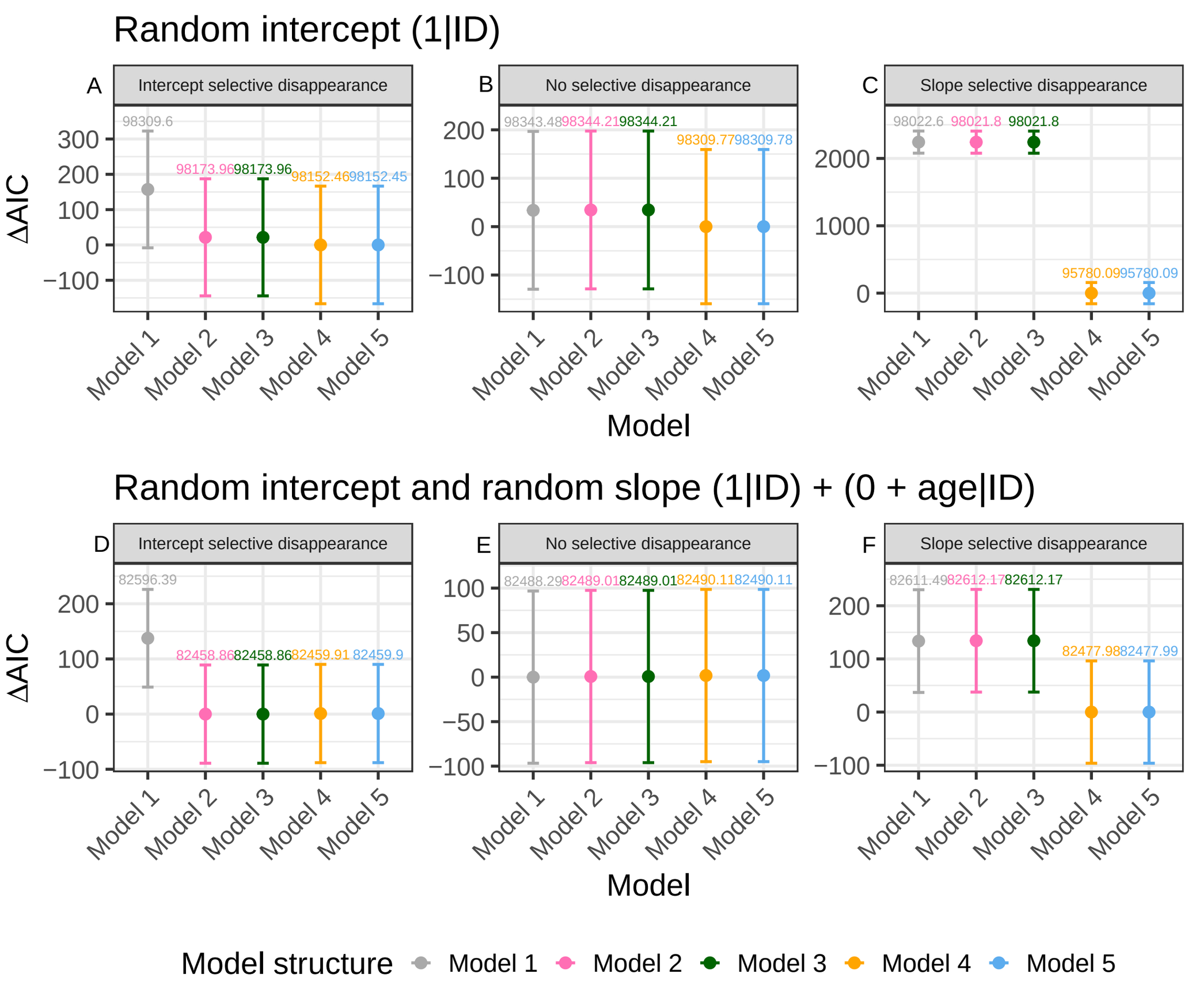
Random intercept (1|ID)
A
Intercept selective disappearance
B
No selective disappearance
C
Slope selective disappearance
ΔAIC
98309.6
98173.96 98173.96 98152.46 98152.45
98343.48 98344.21 98344.21 98309.77 98309.78
98022.6 98021.8 98021.8 95780.09 95780.09
Model 1
Model 2
Model 3
Model 4
Model 5
Model
Random intercept and random slope (1|ID) + (0 + age|ID)
D
Intercept selective disappearance
E
No selective disappearance
F
Slope selective disappearance
82596.39
82458.86 82458.86 82459.91 82459.9
82488.29 82489.01 82489.01 82490.11 82490.11
82611.49 82612.17 82612.17 82477.98 82477.99
Model structure
Model 1
Model 2
Model 3
Model 4
Model 5

A
Int: 0 ; Slope: 0 ; Shape: 0
29.3
30.5
30.5
0
3.3
100
0
−100
B
Int: 0.5 ; Slope: 0 ; Shape: 0
165.5
39.5
67.4
0
36
300
200
100
0
−100
C
Int: −0.5 ; Slope: 0 ; Shape: 0
135.5
15.9
43.6
0
32.2
300
200
100
0
−100
D
Int: 0 ; Slope: 0.5 ; Shape: 0
449.3
447.1
447.9
138.8
0
500
250
0
E
Int: 0 ; Slope: −0.5 ; Shape: 0
451.2
449.2
449.8
131.6
0
500
250
0
F
Int: 0 ; Slope: 0 ; Shape: 0.5
402.8
403.3
403.2
131.5
0
600
400
200
0
G
Int: 0 ; Slope: 0 ; Shape: −0.5
436
436.4
436.5
157
0
600
400
200
0
H
Int: 0.5 ; Slope: 0.5 ; Shape: 0.5
2456
2247.7
2303.9
916.7
0
2000
1000
0
I
Int: −0.5 ; Slope: −0.5 ; Shape: −0.5
2338.4
2120.1
2177.8
910.3
0
2000
1000
0
ΔAIC
Model 1
Model 2
Model 3
Model 4
Model 5
Model

A

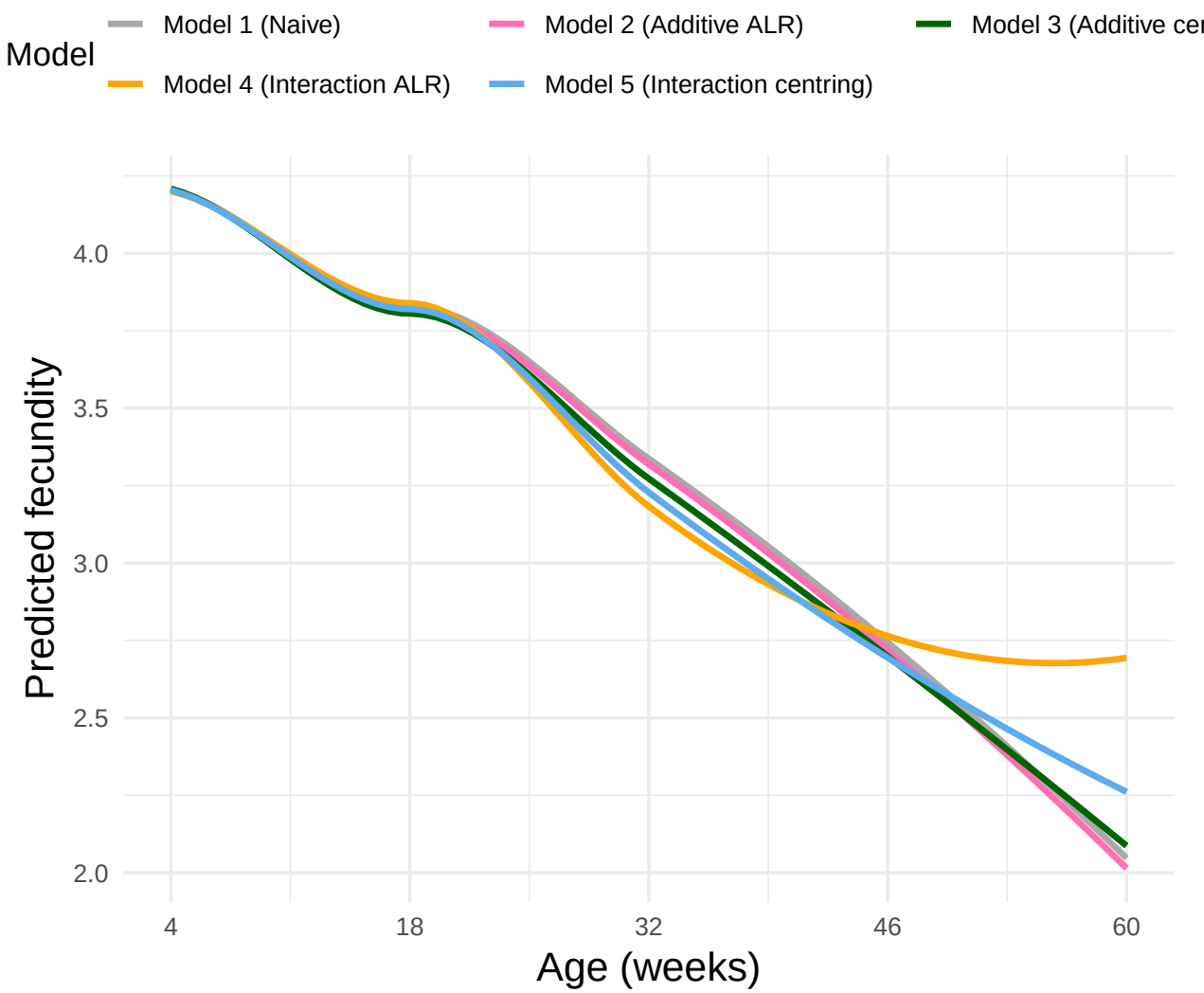
Model
Model 1 (Naive)
Model 2 (Additive ALR)
Model 3 (Additive centring)
Model 4 (Interaction ALR)
Model 5 (Interaction centring)
Predicted fecundity
4.0
3.5
3.0
2.5
2.0
4
18
32
46
60
Age (weeks)

B

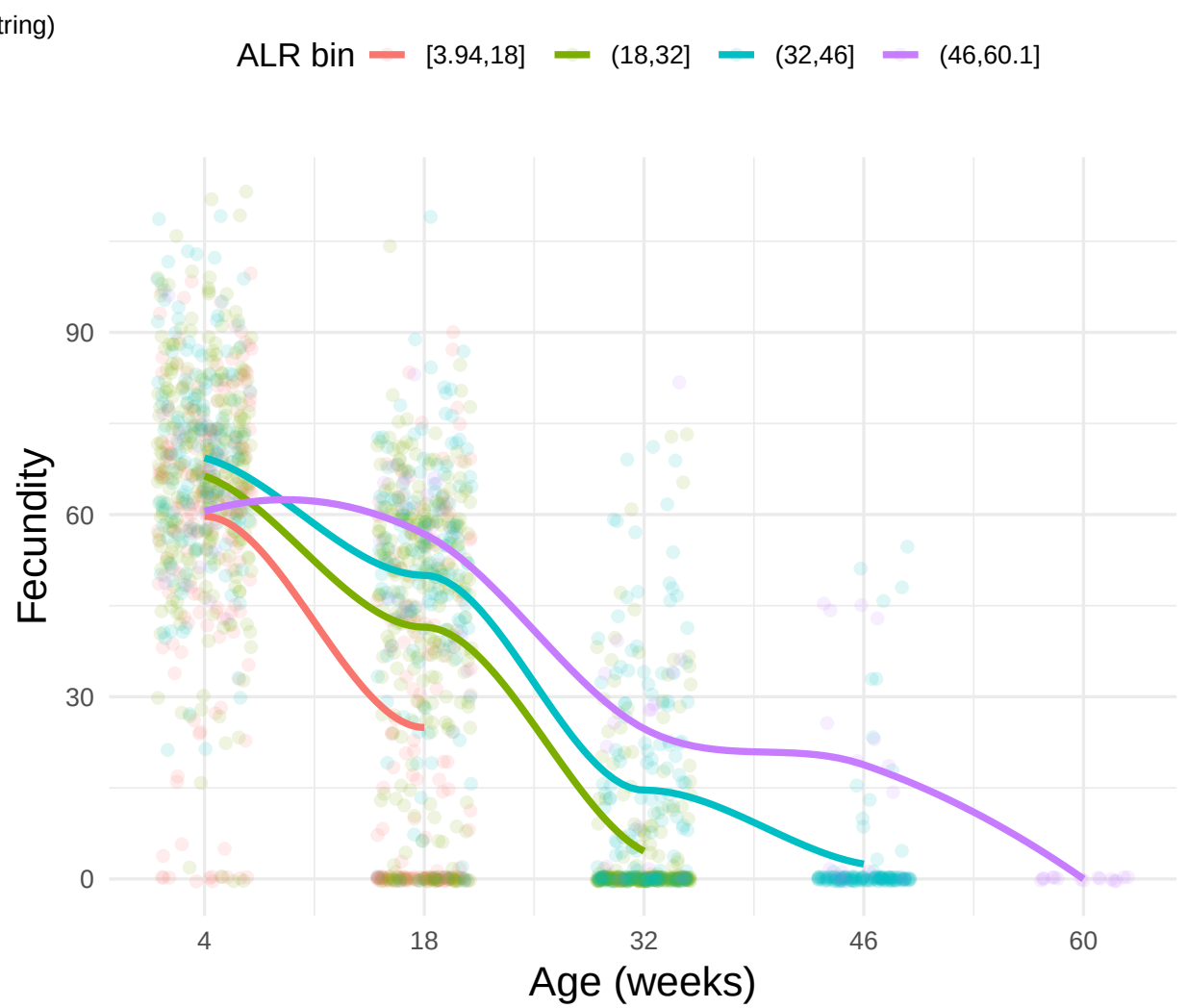
ALR bin
[3.94,18]
(18,32]
(32,46]
(46,60.1]
Fecundity
90
60
30
0
4
18
32
46
60
Age (weeks)

C

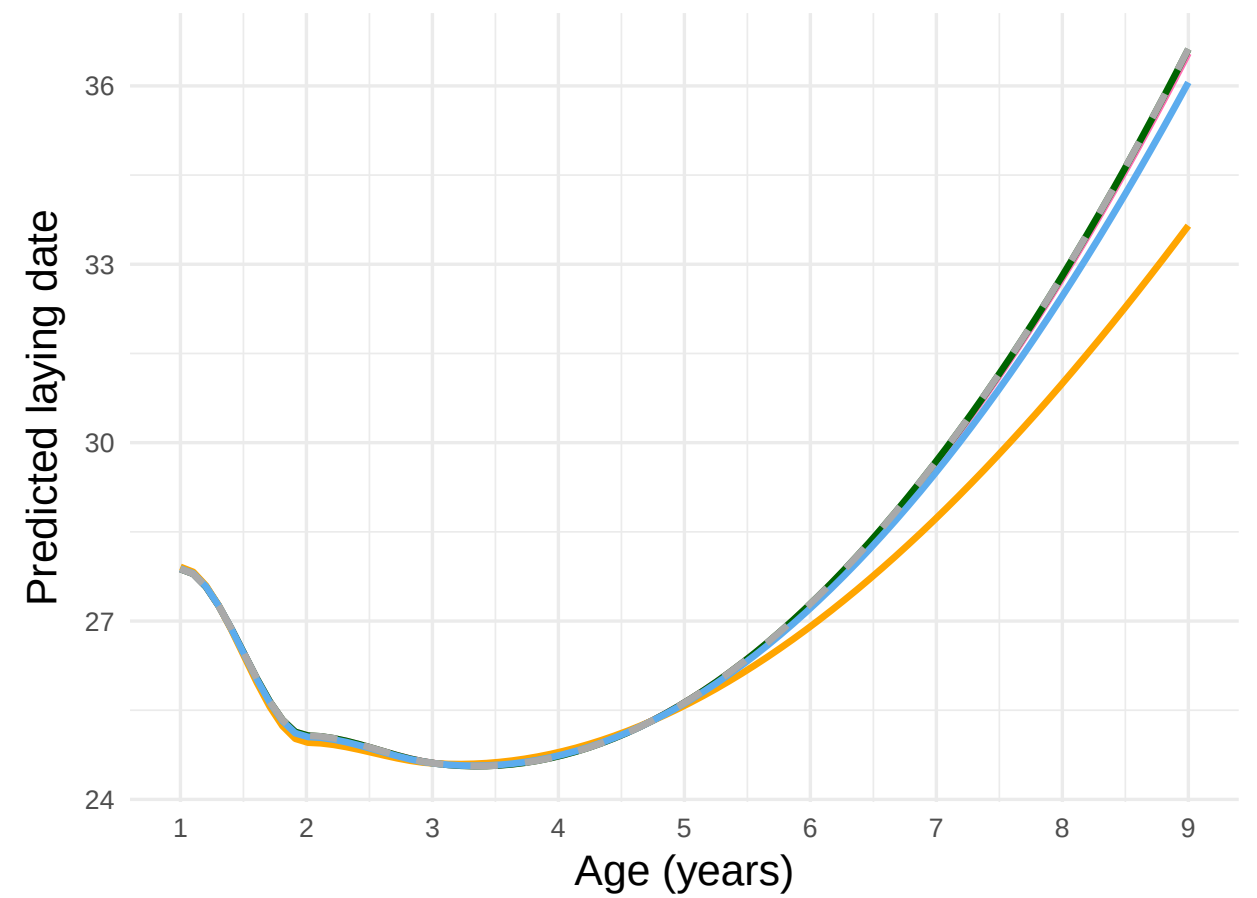
Predicted laying date
36
33
30
27
24
1
2
3
4
5
6
7
8
9
Age (years)

D

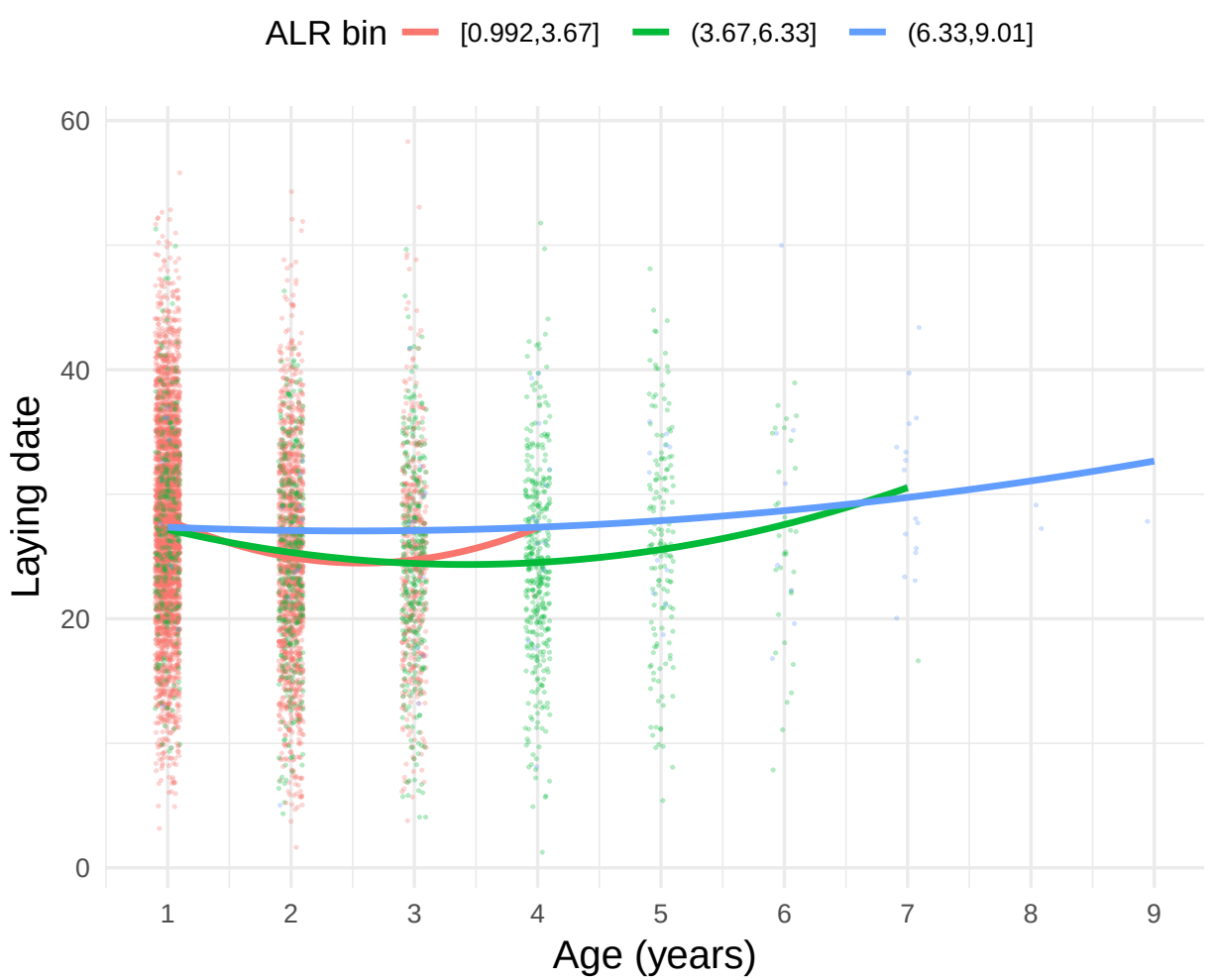
ALR bin
[0.992,3.67]
(3.67,6.33]
(6.33,9.01]
Laying date
60
40
20
0
1
2
3
4
5
6
7
8
9
Age (years)

Supplementary sections S1-S4

1 Supplementary section S1- Analytical solutions

Younger age classes often contain a mix of long- and short-lived individuals. However, old age classes, by definition, contain longer-lived individuals only. Therefore, as populations age, there is generally a bias in the longevity of the sampled population (Sanghvi et al, 2024b; Vaupel and Yashin, 1985). While researchers are interested in quantifying ageing in a trait, the observed pattern emerges not only due to effects of age on that trait directly, but also due to selection on lifespan and its covariance with the trait of interest- which is the mechanism of selective disappearance. Based on this, we derive analytical solutions to quantify: (i) how selective disappearance causes within- and among-individual ageing trajectories to diverge; (ii) how selective disappearance impacts the calculation of the decomposition method; and (iii) what variables impact the rate of change of the bias caused by selective disappearance. Like in our main text, we use 'fecundity' as the hypothetical age-dependent trait, but our solutions are valid for any longitudinally sampled, non-survival trait.

1.1 Fecundity-determining variables

For simplicity, we assume that individuals follow a quadratic trajectory of ageing, where lifespan (LS) and the three fecundity-determining random variables ($\beta_0, \beta_1, \beta_2$) are drawn from a multivariate normal distribution. Here, the fecundity value at a specific age (or discrete time step, t), F_t, is a time-dependent linear combination of these:

$$F_t = \beta_0 + \beta_1 t + \beta_2 t^2 \tag{1}$$

Because covariance is a linear operator (i.e. $Cov(X, aY + bZ) = aCov(X, Y) + bCov(X, Z)$), the covariance between LS and fecundity at age t is the sum of the covariances of the three individual random variables that collectively determine fecundity (β_0, β_1, and β_2), and LS. This can be written as:

$$Cov(LS, F_t) = Cov(LS, \beta_0) + t \cdot Cov(LS, \beta_1) + t^2 \cdot Cov(LS, \beta_2) \tag{2}$$

This equation represents that at any given age, the covariance between lifespan and fecundity has an age-independent component, and an age-dependent component. Here, if only the $Cov(LS, \beta_0)$ term is non-zero, the association between lifespan and fecundity will remain the same across all ages. However, if $Cov(LS, \beta_1)$ or $Cov(LS, \beta_2)$ are non-zero, the relationship between LS and the expressed/sampled fecundity (F_t) will change systematically and dynamically as individuals age. Covariances can be written as a product of the correlation (ρ) and the standard deviations (σ). Thus, the covariance between LS and any of the other three random variables can be expressed as:

$$Cov(LS, \beta_x) = \sigma_{LS,\beta_x} = \rho_{LS,\beta_x} \cdot \sigma_{LS} \cdot \sigma_{\beta_x} \tag{3}$$

1.2 Derivation of the deviation

At a given age t, we are interested in the difference between the population-level expected fecundity, $E[F_t]$, and the fecundity observed in the surviving individuals. To quantify the mechanism of selective disappearance, we can model the fecundity of an individual (F_t) by adjusting for how its lifespan deviates from the population average. In

a linear regression framework where both LS and F_t are treated as random variables, this relationship is expressed as:

$$F_t = E[F_t] + \beta_{LS}(LS - \mu_{LS}) + \epsilon \tag{4}$$

Here, the population's baseline fecundity ($E[F_t]$) is adjusted by the individual's longevity deviation ($LS - \mu_{LS}$), scaled by the regression coefficient β_{LS}. The term ϵ represents the residual variation in fecundity that is uncorrelated with lifespan. When data is truncated, the conditional expectation of the outcome shifts as a function of selection on the truncated variable. Because observing fecundity at age t for an individual is conditional on the individual surviving to that age ($LS \geq t$), applying this conditional expectation gives:

$$E[F_t|LS \geq t] = E[F_t] + \beta_{LS} \cdot E[LS - \mu_{LS}|LS \geq t] + E[\epsilon|LS \geq t] \tag{5}$$

where $E[F_t]$ represents the true population mean at age t; the term $\beta_{LS} \cdot E[LS - \mu_{LS} \mid LS \geq t]$ represents the bias introduced by the covariance between lifespan and fecundity, scaled by the shift in mean lifespan among survivors; and $E[\epsilon|LS \geq t]$ is the expected value of the residuals among survivors.

Under the assumption of a multivariate normal distribution, the residuals (ϵ) are independent of the predictor (LS); consequently, $E[\epsilon \mid LS \geq t] = E[\epsilon] = 0$. For a normal distribution, the expected shift of a truncated variable can be expressed as:

$$E[LS - \mu_{LS} \mid LS \geq t] = \sigma_{LS} \cdot \lambda(\alpha_t) \tag{6}$$

where $\lambda(\alpha_t)$ is the Inverse Mills ratio (Heckman, 1979) at the truncation point α_t. Here, $\alpha_t = (t - \mu_{LS})/\sigma_{LS}$ represents the standardized age (or Z-score). Biologically, this expresses the number of standard deviations that the chronological age t is from the mean lifespan. This normalizes the mortality trajectory so that the intensity of selective disappearance depends on the cohort's relative position within the lifespan distribution rather than absolute (chronological) time. The Inverse Mills ratio at t is calculated as $\lambda(\alpha_t) = \frac{\phi(\alpha_t)}{1-\Phi(\alpha_t)}$. Here, ϕ represents the standard normal probability density function (PDF), reflecting the relative likelihood of death at age t, while Φ represents the standard normal cumulative distribution function (CDF), representing the proportion of the population that has died by that age. Our assumption of normally distributed lifespans when substituting the Inverse Mills ratio has only been done for convenience and simplicity, and Weibull or Gompertz distributions can also be used instead. For an ordinary least squares regression, the regression coefficient is expressed as $Cov(X, Y)/\sigma_X^2$. Thus we can substitute for β_{LS} as $Cov(LS, F_t)/\sigma_{LS}^2$, and further substituting Eq. 6 into Eq. 5 gives:

$$E[F_t|LS \geq t] - E[F_t] = \frac{Cov(LS, F_t)}{\sigma_{LS}^2} \cdot \sigma_{LS} \cdot \lambda(\alpha_t) \tag{7}$$

Here, $E[F_t|LS \geq t] - E[F_t]$ represents the deviation between the observed fecundity of the surviving population and the true expected fecundity, at a given age, henceforth referred to as the deflection (or deviation)- '$D(t)$'. By canceling the σ_{LS} terms, we obtain:

$$D(t) = \frac{\lambda(\alpha_t)}{\sigma_{LS}} Cov(LS, F_t) \tag{8}$$

Here, the term $\frac{\lambda(\alpha_t)}{\sigma_{LS}}$ represents the mortality hazard rate (selection intensity) at age t. This equation can be further rewritten by substituting for $Cov(LS, F_t)$ (from Eq. 2) as: $D(t) = \frac{\lambda(\alpha_t)}{\sigma_{LS}}(Cov(LS, \beta_0) + t \cdot Cov(LS, \beta_1) + t^2 \cdot Cov(LS, \beta_2))$. Substituting for covariances from Eq. 3, and canceling out the common σ_{LS}, we get the final solution:

$$D(t) = \lambda(\alpha_t) \cdot (\rho_{LS,\beta_0} \cdot \sigma_{\beta_0} + t \cdot \rho_{LS,\beta_1} \cdot \sigma_{\beta_1} + t^2 \cdot \rho_{LS,\beta_2} \cdot \sigma_{\beta_2}) \tag{9}$$

Equation 8 provides a crucial biological insight- that the magnitude of the deviation at an age t depends on the product of two processes: (i) the selection intensity on mortality (hazard rate) at that age; and (ii) the total

covariance between lifespan and fecundity at that age. Equation 9 provides several additional biological insights. First, it shows that observed changes in fecundity with age can arise entirely independent of within-individual changes with age, i.e. when β_1 or β_2 are zero. Second, even under the absence of correlations between LS and the intercept, we can get selective disappearance due to correlations between LS, and slope or shape. Third, the bias caused by selective disappearance increases with age for two reasons: (i) because the selection intensity on lifespan, $\lambda(\alpha_t)$, increases with age; and (ii) at later ages, the effects of $\rho_{LS,\beta_1} \cdot \sigma_{\beta_1}$ and $\rho_{LS,\beta_2} \cdot \sigma_{\beta_2}$ get multiplied by t and t^2 respectively. Due to this, even weak correlations between LS and slope or shape can lead to dramatic selective disappearance effects at later ages (Figures S53-S55). Fourth, the magnitude of selective disappearance at an age t scales with the among-individual variability of the fecundity variables (i.e. σ_{β_X}). However, it does not scale with the among-individual variability in lifespan, σ_{LS}. Specifically, when if compare two populations with different lifespan variances at the same *standardized* age (e.g. when both have reached the 90th percentile of the lifespan distribution), the magnitude of deviation will be identical because the σ_{LS} term cancels out.

1.3 Why the decomposition method is biased

We can quantify how the decomposition method estimates within-individual change, and why this is different from the 'true', underlying, overall within-individual change across individuals. For this, lets assess the change in the trait over two discrete time steps (i.e. from t to $t+1$). The 'true change' ($\Delta E[F_t]$) is:

$$\begin{aligned} \Delta E[F_t] &= E[F_{t+1}] - E[F_t] \qquad (10) \\ &= [\beta_0 + \beta_1(t+1) + \beta_2(t+1)^2] - [\beta_0 + \beta_1 t + \beta_2 t^2] \\ &= \beta_1 + \beta_2(2t+1) \qquad (11) \end{aligned}$$

Note that the change over one time step is independent of the intercept (β_0) and depends only on the slope (β_1) and shape (β_2). Now lets consider the change over this time step as estimated by the decomposition method (ΔI_t). The decomposition method estimates the within-individual change by restricting the analysis only to the cohort of individuals that survive the interval (i.e. those alive at both t and $t+1$, conditional on $LS \geq t+1$). Therefore:

$$\Delta I_t = E[F_{t+1} \mid LS \geq t+1] - E[F_t \mid LS \geq t+1] \qquad (12)$$

Using the conditional expectation formula (see Eq. 5, 6, 7), we can expand both terms:

$$\begin{aligned} \Delta I_t &= \left(E[F_{t+1}] + \frac{\lambda(\alpha_{t+1})}{\sigma_{LS}} Cov(LS, F_{t+1})\right) - \left(E[F_t] + \frac{\lambda(\alpha_{t+1})}{\sigma_{LS}} Cov(LS, F_t)\right) \\ &= \underbrace{(E[F_{t+1}] - E[F_t])}_{\text{True change}} + \underbrace{\frac{\lambda(\alpha_{t+1})}{\sigma_{LS}}\Big[Cov(LS, F_{t+1}) - Cov(LS, F_t)\Big]}_{\text{Bias of decomposition method}} \qquad (13) \end{aligned}$$

Note that a bias in the decomposition method arises because the decomposition method analyzes the *same* set of survivors for both time points. Therefore, the selection intensity at both time steps is treated as the selection intensity at $t+1$, leading to the covariance at time t being scaled by $\lambda(\alpha_{t+1})$ rather than $\lambda(\alpha_t)$. We can further expand and simplify the difference between the covariance terms in '[ ]' by substituting Eq. 2, which gives us:

$$Cov(LS, F_{t+1}) - Cov(LS, F_t) = \sigma_{LS}\left(\rho_{LS,\beta_1}\sigma_{\beta_1} + (2t+1)\rho_{LS,\beta_2}\sigma_{\beta_2}\right) \qquad (14)$$

Substituting Eq. 14 back into Eq. 13 and simplifying gives us:

$$\Delta I_t = \text{'True change'} + \underbrace{\lambda(\alpha_{t+1})\left(\rho_{LS,\beta_1}\sigma_{\beta_1} + (2t+1)\rho_{LS,\beta_2}\sigma_{\beta_2}\right)}_{\text{Bias of decomposition method}} \qquad (15)$$

Equation 15 gives us two important insights (Figure S56). First, the decomposition method's bias is independent of the intercept (i.e. of ρ_{LS,β_0} and σ_{β_0}). Second, the decomposition bias is specifically associated with selective disappearance linked to the trait's slope and/or shape, i.e. ρ_{LS,β_1} and ρ_{LS,β_2}, and their variability (σ_{β_1} and σ_{β_2}). Here, the decomposition bias becomes exacerbated with age for two reasons: (i) $\lambda(\alpha_t)$ increases with age; (ii) the correlation between lifespan and shape, $\rho_{LS,\beta_2}\sigma_{\beta_2}$, is multiplied with time t. These analytical insights corroborate with our simulation results where under selective disappearance linked with the trait's slope or shape, the decomposition method is inaccurate especially at later ages (Figure 1D-1I); however, under selective disappearance only linked with the intercept (or no selective disappearance), it is accurate (Figure 1B and 1C).

1.4 Observed versus decomposition

For two discrete time steps, we can calculate the observed population-level change in the trait's value (ΔP_t) over this time step. The observed change compares the mean of *all* survivors at $t+1$ to the mean of *all* survivors at t. Thus, unlike the decomposition method, here the pool of individuals can change between the two time steps if some individuals die:

$$\Delta P_t = \underbrace{E[F_{t+1} \mid LS \geq t+1]}_{P_{t+1}} - \underbrace{E[F_t \mid LS \geq t]}_{P_t} \tag{16}$$

Note that the term, $P_{t+1} = E[F_{t+1} \mid LS \geq t+1]$, can be related to the decomposition method by rearranging and substituting Eq. 12 as:

$$P_{t+1} = E[F_{t+1} \mid LS \geq t+1] = \Delta I_t + E[F_t \mid LS \geq t+1] \tag{17}$$

Substituting this back into Eq. 16:

$$\Delta P_t = \Delta I_t + E[F_t \mid LS \geq t+1] - E[F_t \mid LS \geq t] \tag{18}$$

We can further expand the two conditional expectation terms (see Eq. 5, 6, 7) as:

$$E[F_t \mid LS \geq t+1] - E[F_t \mid LS \geq t] = \left(E[F_t] + \frac{\lambda(\alpha_{t+1})}{\sigma_{LS}} Cov(LS, F_t)\right) - \left(E[F_t] + \frac{\lambda(\alpha_t)}{\sigma_{LS}} Cov(LS, F_t)\right) \tag{19}$$

Substituting this in Eq. 18 and simplifying gives us:

$$\Delta P_t = \Delta I_t + \underbrace{(\lambda(\alpha_{t+1}) - \lambda(\alpha_t))}_{\Delta\lambda \text{ (Selection acceleration)}} \cdot \frac{Cov(LS, F_t)}{\sigma_{LS}} \tag{20}$$

Eq. 20 shows that the observed population-level change in the trait's value across two discrete time steps not only includes the change as estimated by the decomposition method (i.e. ΔI_t), but also additionally includes a 'Selection acceleration' ($\Delta\lambda$) term. This term quantifies how mortality selection is changing over the time step. Because the mortality hazard rate typically increases with age ($\lambda(\alpha_{t+1}) > \lambda(\alpha_t)$), this term creates a 'drift' in the observed population trajectory, and explains why the observed trajectory deviates more (and earlier) from the true trajectory compared to the decomposition trajectory's deviation (as seen in our results, e.g. Figure 2).

This equation provides another crucial insight regarding the role of lifespan variability (σ_{LS}). When the term $\frac{Cov(LS,F_t)}{\sigma_{LS}}$ is expanded and simplified, σ_{LS} cancels out (as seen in Eq. 8 and 9), confirming that variability in LS does not impact the magnitude of the bias. However, σ_{LS} impacts the *rate of change* of the deviation via the selection acceleration term. This is because the standardized age is defined as $\alpha_t = (t - \mu_{LS})/\sigma_{LS}$. Consequently, the difference in the standardized age between two consecutive time steps is:

$$\alpha_{t+1} - \alpha_t = \frac{t+1-\mu_{LS}}{\sigma_{LS}} - \frac{t-\mu_{LS}}{\sigma_{LS}} = \frac{1}{\sigma_{LS}} \tag{21}$$

Therefore, σ_{LS} contributes towards the selection acceleration term and inversely scales with the "step size" along the mortality curve. In populations with low lifespan variability (small σ_{LS}), the step size $1/\sigma_{LS}$ will be large, thus the difference between $\lambda(\alpha_{t+1})$ and $\lambda(\alpha_t)$ will be high. This will cause a rapid acceleration in the bias (high rate of change in deviation) with age when variability in lifespan in a population is low. In contrast, populations with high variability in lifespans will experience a gradual change in the deviation over time (see Figure S57, S58 for a visualization of this).

1.5 Comparison of analytical and simulation results

To show that our simulations are robust and supported by our analytical solutions, we calculate how selective disappearance of slope, shape, and intercept, impact the deviation between the observed and the true pattern, using Eq. 8 and 9 above. For the entire range of simulated lifespans, these calculations can be found in the 'Analytical solution' section of our R code. As proof of concept of the calculations, for three arbitrarily chosen time points, we show these calculations by hand, and these can be found in Supplementary data: 'Analytical calculation data' uploaded on OSF (https://osf.io/kevnm/overview?view_only=93eba71a58444d19b5fb5287ffbc61e4). Comparisons between the analytically calculated deviation and the deviation observed in the simulations can be found in Figure 2 and Figure S12.

1.6 References

Heckman, J. J. (1979). Sample Selection Bias as a Specification Error. *Econometrica*, 47(1), 153. https://doi.org/10.2307/1912352

2 Supplementary section S2- Model, method precision

We compared the precision of the different statistical models and the decomposition method. This was done to test whether the more complex models, 4 and 5, were less precise (i.e. higher variance in predicted fecundity between replicates) due to overfitting or having a low 'sample size:fixed effects' ratio. To quantify this, we calculated a 'relativized precision' metric for each model and the decomposition method, separately for each scenario. First, for every age within a specific scenario, we calculated the standard deviation of the predicted fecundity values across the $N = 50$ replicates as:

$$\sigma_{\texttt{prediction,age}} = \sqrt{\frac{\sum_{r=1}^{N}(\hat{P}_{\texttt{rep,age}} - \bar{F}_{\texttt{age}})^2}{N-1}} \tag{22}$$

where $\hat{P}_{\texttt{rep,age}}$ is the predicted value of fecundity for a replicate at a given age, by a model. To make the $\sigma_{\texttt{prediction,age}}$ comparable across models, we relativized it by the magnitude of the age effect predicted by the model. Specifically, for each replicate we calculated the range of the predicted trajectory:

$$\texttt{Range}_{\texttt{rep}} = \max(\hat{P}_{\texttt{rep}}) - \min(\hat{P}_{\texttt{rep}}) \tag{23}$$

We then averaged these ranges across the 50 replicates to obtain the mean range for that model and that scenario ($\overline{\texttt{Range}}$). Finally, we calculated the relativized precision by dividing the age-specific $\sigma_{\texttt{prediction,age}}$ by the mean prediction range. This provided a noise-to-signal ratio such that higher values indicated lower precision relative to the strength of the predicted biological signal. This was done as:

$$\text{Relativized precision}_{\texttt{age}} = \left(\frac{\sigma_{\texttt{prediction,age}}}{\overline{\texttt{Range}}}\right) \times 100 \tag{24}$$

We calculate relativized precision for the decomposition method too using Eq. 22-24, however, replacing the "predicted" fecundity value at each age by the fecundity as estimated by the decomposition method for that age and replicate. Note that these calculations were done separately for each scenario.

3 Supplementary section S3- Sensitivity analyses

We conducted various sensitivity analyses (Figure 1E). All sensitivity analyses included calculations of deviation between the observed and decomposition trajectories, comparisons of model AICs and model/method predictions. Sensitivity analyses were conducted under complete sampling (i.e. no missingness) and parameterized for lifespans being sampled from normal distributions with a μ_{LS} of 25 time steps, unless mentioned otherwise.

3.1 Onset of ageing

To test whether our simulations were sensitive to how different traits were parametrized, thus the pace and shape of ageing, we changed the mean values of β_1 and β_2 to reflect slow ($\mu_{\beta_1} = 9$; $\mu_{\beta_2} = -0.2$) and fast ($\mu_{\beta_1} = 5$; $\mu_{\beta_2} = -0.3$) ageing.

3.2 Sample size

Larger sample sizes could have levied a lower relative penalty on the AIC calculation of more complex models. Furthermore, smaller sample sizes could lead to greater imprecision of interaction terms. To test this, instead of simulating 250 individuals, we conducted a sensitivity analysis simulating only 50 individuals, per replicate.

3.3 Few time steps (short-lived species)

To test whether our results held true when a species with only few time steps of average lifespan was simulated, instead of parameterizing μ_{LS} as 25 time steps, we changed this value to 5 (Figure S8). To keep the relative trajectory of ageing the same as our complete sampling simulation, we scaled the linear and quadratic coefficients by 5 and 5^2 respectively (also see Figure 1E). This sensitivity analysis could thus represent an annually sampled species that lives up to 5 years on average, but has a fast life-history strategy. This sensitivity analysis of five simulated time steps was done for both, the complete sampling as well as the missing completely at random (MCAR) simulations. It was also done for lifespan not only being sampling from a normal distribution, but also from a Gamma distribution in separate simulations (see section 3.4 below).

3.4 Gamma distribution of lifespan

Instead of sampling lifespan from a normal distribution, we sampled it from a right skewed Gamma distribution. This was done to reflect high mortality in early life and only few individuals surviving to older ages, as is often the case in wild populations. For the Gamma distributed simulation, we employed both, the complete sampling as well as MCAR (50% missing) simulation structure. Additionally, we conducted this simulation for both, the longer-lived species as in our complete sampling simulation (μ_{LS} = 25 time steps), and for the shorter-lived species (μ_{LS} = 5 time steps) (see Figures S9, S10).

To create correlations between normally distributed fecundity variables and Gamma distributed LS, we employed a Gaussian copula method, which separates the simulation of the correlation structure from the simulation of the marginal distributions. The Gamma distribution is parameterized by a shape (α) and a scale (θ). We first defined these variables as we would for a normal distribution, i.e. based on the mean (μ_{LS}) and standard deviation (σ_{LS}). We then converted these parameters to scale and shape using the method of moments:

$$\alpha = \frac{\mu_{LS}^2}{\sigma_{LS}^2} \quad \text{and} \quad \theta = \frac{\sigma_{LS}^2}{\mu_{LS}} \tag{25}$$

We simulated an intermediate set of four traits from a multivariate normal distribution using the same mean vector

$\boldsymbol{\mu}$ and variance-covariance matrix $\boldsymbol{\Sigma}$ as described in our methods. Next, we transformed each of the four correlated normal variates into uniformly distributed variates on the interval [0, 1]. This was done using the Probability Integral Transform (PIT), by applying the standard normal cumulative distribution function (`pnorm` in R) to each simulated value. This preserved the rank correlation (copula) from the previous step while removing the specific marginal properties of the normal distribution.

Finally, we used the inverse transform sampling method to convert the correlated uniform variates into our target distributions. For lifespan, we applied the inverse cumulative distribution function (CDF) of the Gamma distribution (`qgamma` in R) to the first uniform variate, using the shape and scale variables. For the three fecundity variables, we applied the inverse CDF of the Normal distribution (`qnorm` in R) to the remaining three uniform variates. This final step imparted the desired marginal distribution to each trait (Gamma for lifespan, Normal for the others) while retaining the underlying rank-correlation structure. The resulting dataset thus contained individuals with rank-correlated fecundity-LS traits drawn from different distributions.

Compared to our complete sampling simulation, in this sensitivity analysis, we made two parameterization changes. To create a right-skew in the Gamma distributions that emulates high early-life mortality and a long-tail, we parameterized the σ_{LS} as 10, instead of 5. Additionally, to prevent negative values for fecundity at extreme ages, the μ_{β_0} was parametrized to be 2500 instead of 600.

Note that Google AI's- Gemini Pro 3.0 was used to develop the code for the Gaussian Copula method and correlate the random variables from the normal and Gamma distributions. The corresponding author takes full responsibility for the use of AI and has ensured that the code is correct and achieves the desired goal.

4 Supplementary section S4- Empirical data

We [re]analysed data from two studies, to show that insights gained from our simulations were valid for empirical, real-world systems, and that the assumptions made in our simulations about the underlying data did not hinder their applicability.

4.1 Sanghvi et al, 2025

We re-analysed data published by Sanghvi et al, 2025b (Am. Nat). This dataset represents an experiment conducted on a laboratory population of fruit flies, *Drosophila melanogaster*. Their aim was to test how paternal age and paternal sperm storage duration, impact the ageing trajectories of longitudinally sampled offspring. The study contained longitudinally sampled sons' and daughters' reproductive output data, collected once every 2 weeks until the offspring died. It also contained lifespans of nearly all individuals (except some that were left-censored). In their original analysis, the authors used 'model 2' to analyse the ageing of fecundity of offspring born to fathers belonging to one of four treatments. For offspring i born to a father j and at age t, they fit the model:

$$F_{tij} = \beta_0 + \beta_1 \text{age}_{tij} + \beta_2 \text{age}^2_{tij} + \beta_3 \text{LS}_{ij} + \beta_4 \text{Paternal age}_{ij} + \beta_5 \text{Paternal storage}_{ij} + \beta_6 \text{Replicate}_{ij} + u_{0j} + u_{0ij} + \epsilon_{tij} \quad (26)$$

where F_{tij} was modeled with zero-inflated negative binomial error distribution, and LS_{ij} represented the lifespan of each offspring. The study found selective disappearance linked with the intercept in daughters but not sons, i.e. longer-lived daughters have higher fecundity on average, than shorter-lived daughters.

Our goal here was to show that even for studies that account for selective disappearance linked with the intercept using model 2, the within-individual ageing trajectory might be mis-estimated due to these studies not accounting for selective disappearance linked with the trait's shape or slope. We thus re-analysed the data on daughters' reproductive output using GLMMs (glmmTMB package) with a negative binomial error distribution (as in their original study). We implemented models 1-5 as described in our simulation, replacing the age terms with 'offspring age', and replacing the LS term with 'Offspring ALR', to make their models equivalent to models 1-5 in our simulation. In all 5 models, we also included the treatment and environmental variables that were originally used in their study: replicate, paternal age, paternal sperm storage, and paternal fecundity. We then compared these 5 models using AIC, and compared model predictions for the effects of age. As in our simulations, our re-analysis showed that the best fitting model for this dataset was model 4, i.e. the one that included an interaction between ALR and each age term. These data can be found at open science framework `https://osf.io/kevnm/overview?view_only=93eba71a58444d19b5fb5287ffbc61e4` and as Supplementary data in the file- 'Fruit fly data'. Associated analysis can be found in our code under the 'Empirical data' section.

4.2 Bouwhuis et al, 2009

In Bouwhuis et al, 2009, the researchers analyzed how the age of females impacts a suite of traits, such as number of recruits and clutch size. However, in their study, while they had data available on another trait- egg laying date, they did not analyse this. We obtained this data (personal communication between KS and Sandra Bouwhuis, Ben Sheldon on 18/11/2025) and analyzed it using the 5 models as in our simulation. In each model, we additionally included the four environmental variables that they included in their models for the other reported traits: immigrant status of females, nest predation pressure, year's resource quality, and density of individuals. The phenological trait of laying date was continuous and normally distributed, thus our models assumed a Gaussian error distribution. For this dataset too, the best fitting model was the one

analogous to model 4 from our simulations. These data can be found at open science framework https://osf.io/kevnm/overview?view_only=93eba71a58444d19b5fb5287ffbc61e4 and as Supplementary data in the file- 'Great tits data'. Associated analysis can be found in our code under the 'Empirical data' section.